System Modeling and Image Reconstruction for a C-SPECT Scanner

Alfred Hero
EECS Department
University of Michigan
Ann Arbor, MI

Outline

- Overview of Nuclear Medicine
- Tomographic Imaging
  - Analytical methods
  - Statistically based methods
- Compton SPECT
- Reconstruction and Feasibility Analysis

Whole-Body Imaging

- Osteosarcoma, metastatic to lung
- Bone scan with MDP-Tc^{99m}

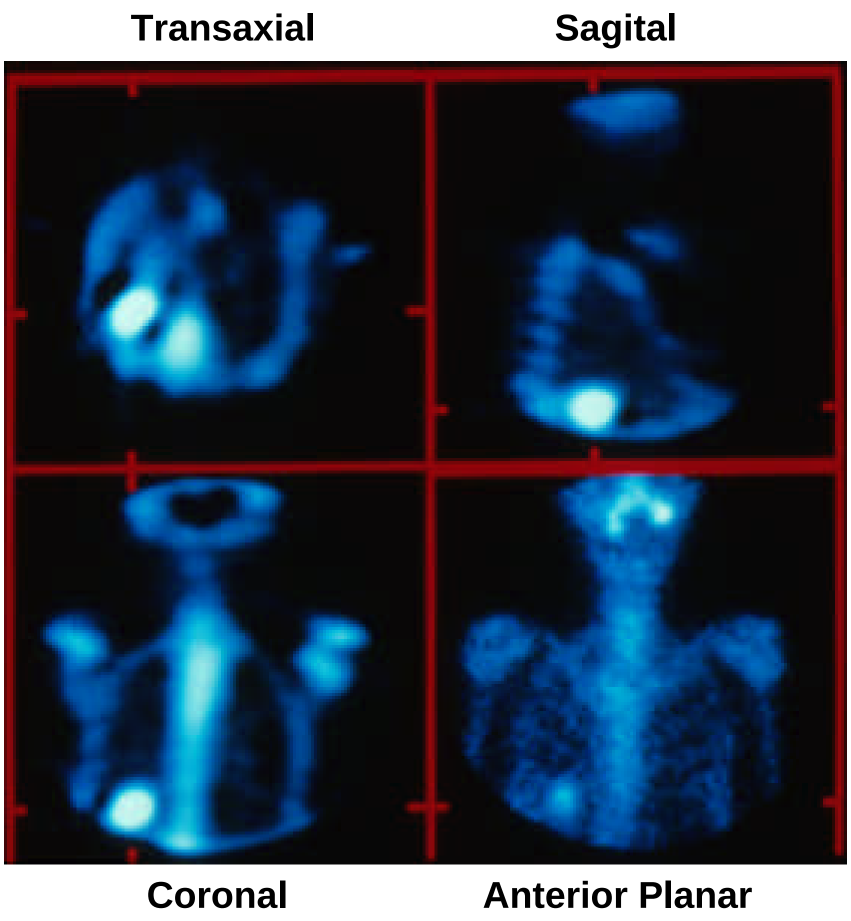

Planar Projection Images

Brain Imaging

- Brain planar projection

Q: Is there reduced blood flow to the left cortex?

Planar Projection Image

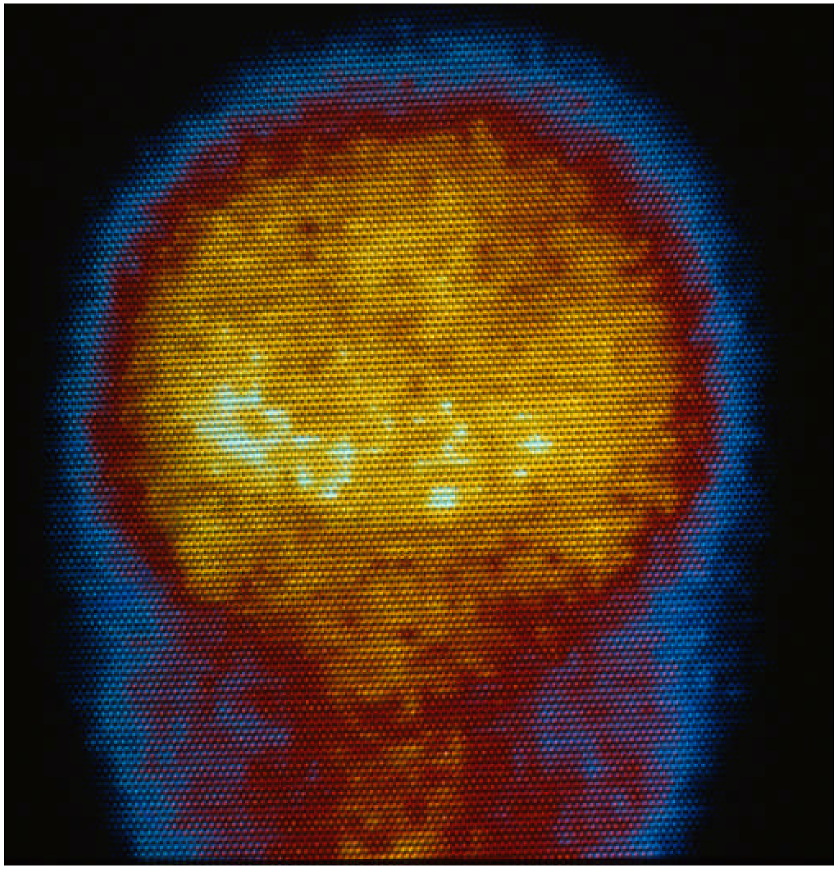

R Anterior View L

Transverse Section

- Brain Transverse Section
- HMPAO blood flow study
- ***Diagnosis: Evidence of stroke in left cortex***

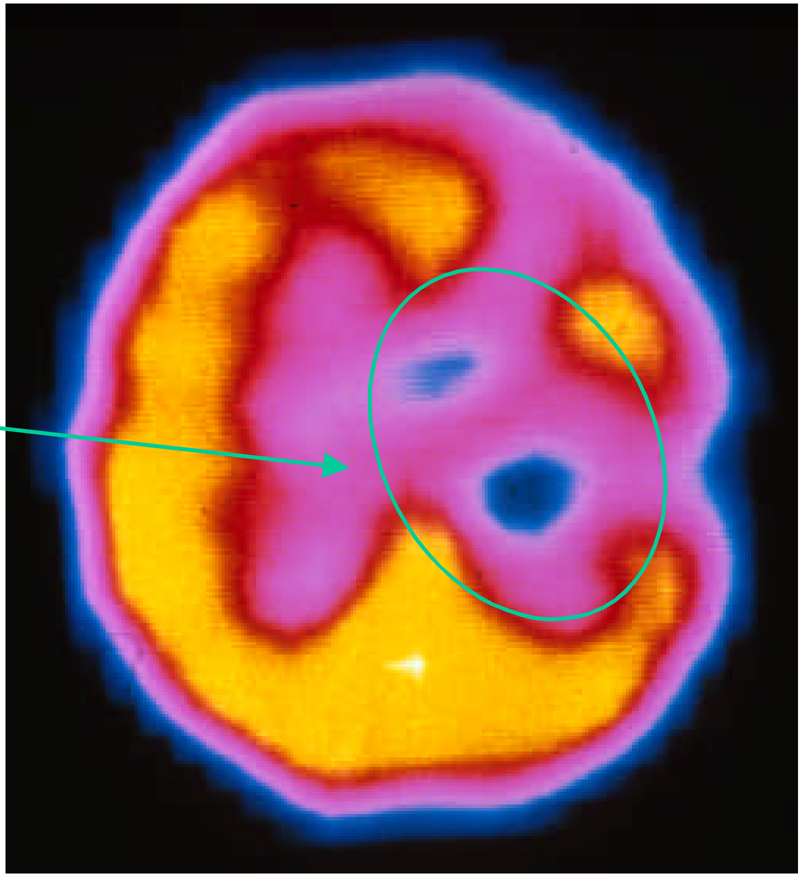

R Transverse Section L

Tomographic Image

Tomographic Brain Imaging

- Brain Transverse Section
- X-Ray CT
- ***Diagnosis: Lesions in left cortex***

Tomographic Image

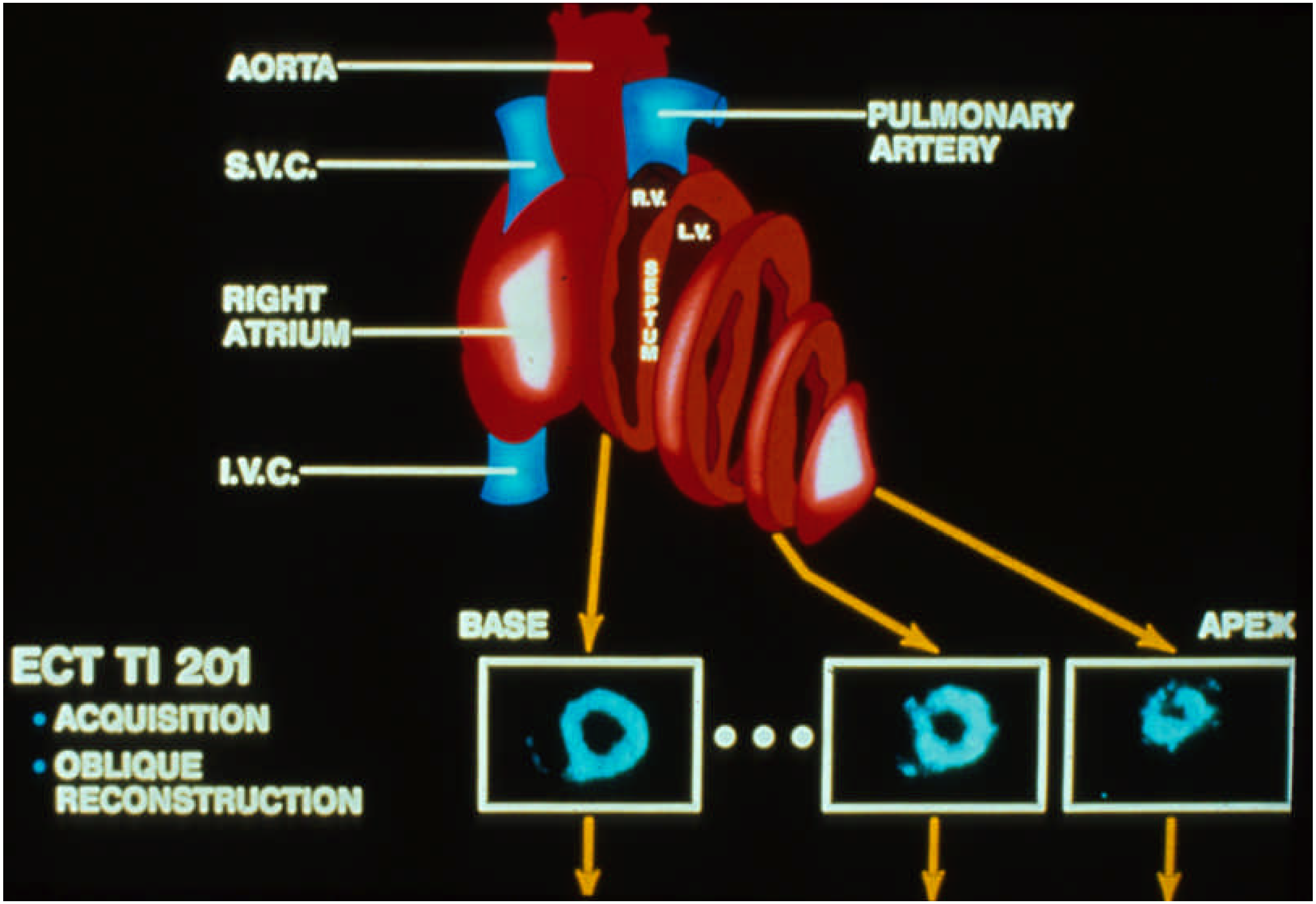
AORTA
PULMONARY ARTERY
S.V.C.
R.V.
L.V.
SEPTUM
RIGHT ATRIUM
I.V.C.
BASE
APEX
ECT Tl 201
• ACQUISITION
• OBLIQUE RECONSTRUCTION

Myocardial Blood Flow
Rest-Stress Study

- Thallium 201
- Myocardial Blood Flow
- Rest-Stress Study
- ***Diagnosis: Interior Wall Ischemia***

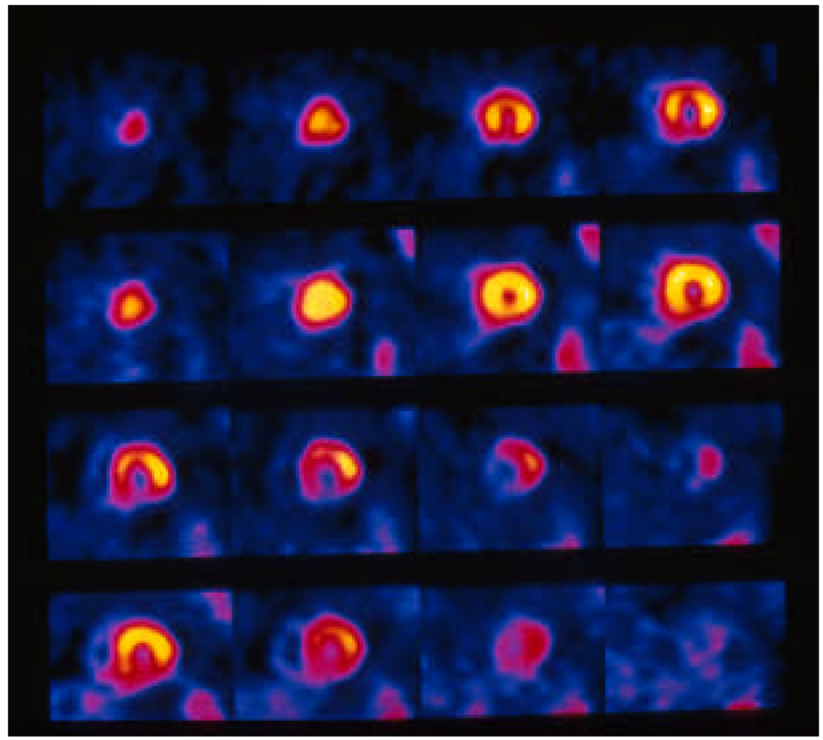

Single Photon Emission Computed Tomography (SPECT)

- 1958 - Anger camera
- 1963 - first ECT device
- 1964 - parallel-hole collimators
- 1972 - statistical image reconstruction
- 1973 - first CT scanner
- Late 70's - first commercial SPECT (Tomomatic)
- 1979 - dual head SPECT & fan-beam collimators
- 1980 - triple head SPECT
- 1984 - ring geometry SPECT
- 90's - combined CT/SPECT and PET/SPECT

Tomographic Imaging: Data Collection

1 **2** **3** **4** **5**

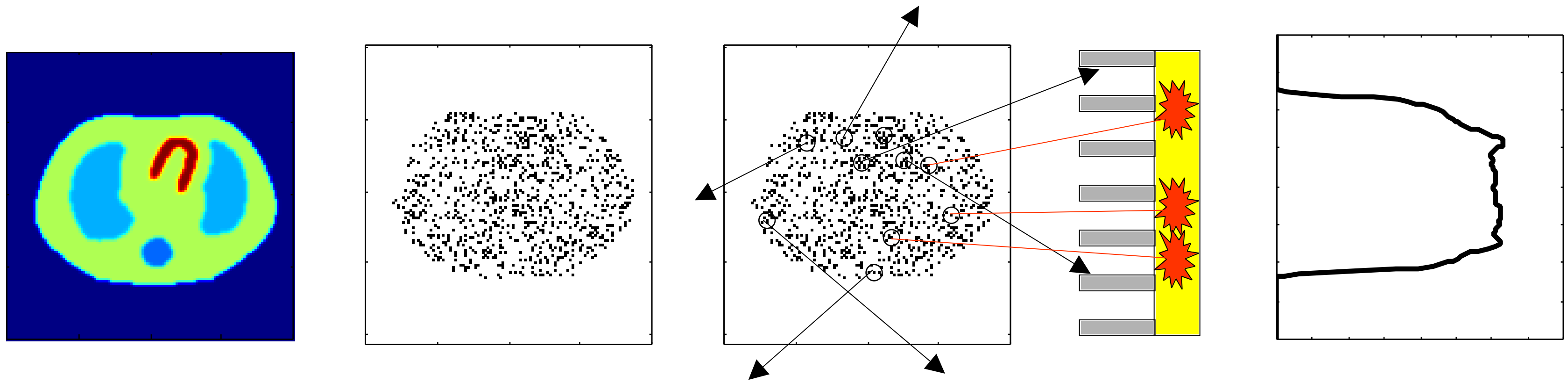

1. Radioactive tracer chemical is ingested by a patient, and concentrates in certain regions...

2. …resulting in a random position distribution of the tracer molecules within the patient’s body...

3. …which undergo radioactive decay, emitting gamma-ray photons in random directions….

4. …some make it through the collimator and are detected...

5. …where the total counts in each bin is proportional to the projection along that axis

Tomographic Imaging: Forward Projections

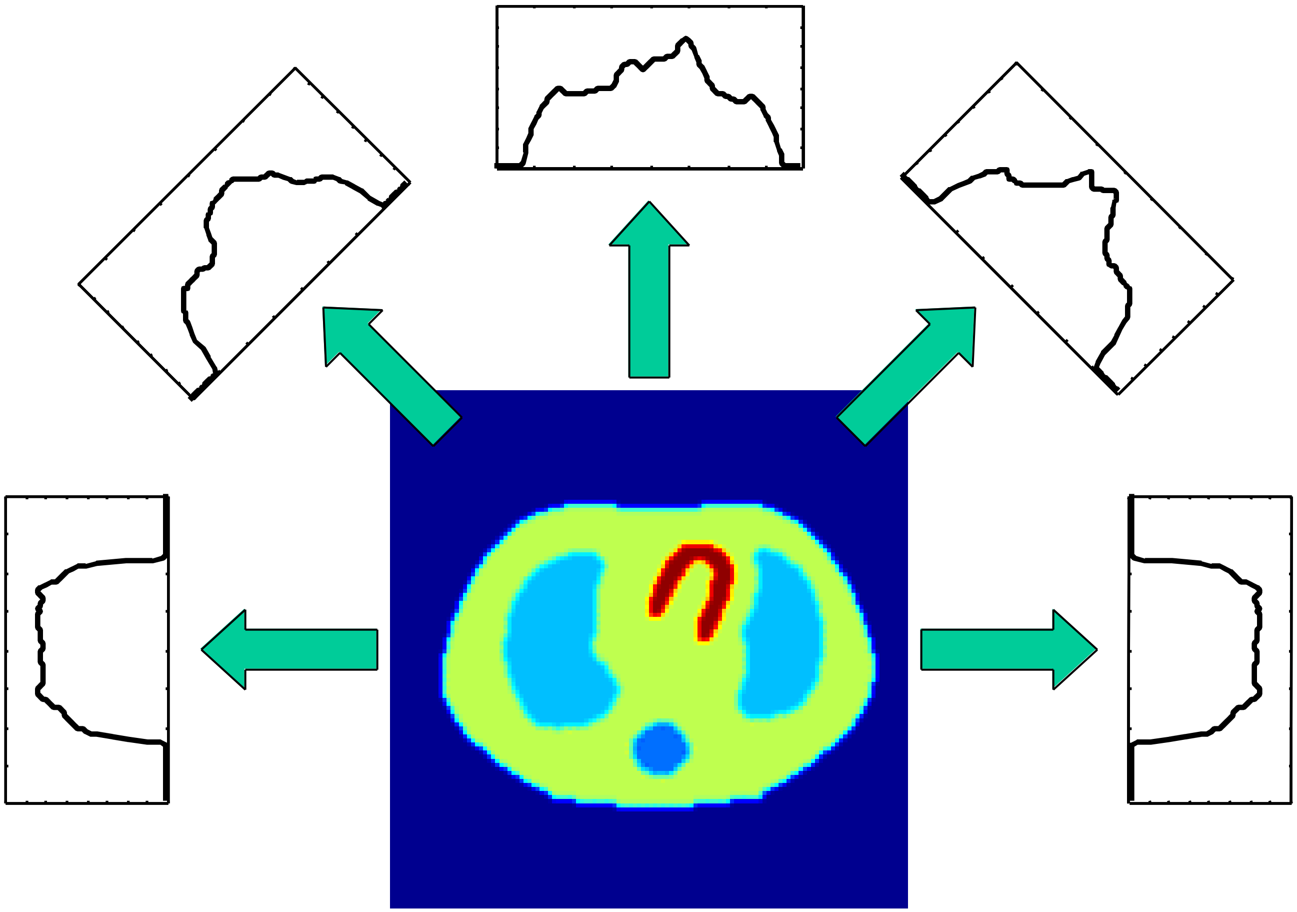

Tomographic Imaging: Back Projections

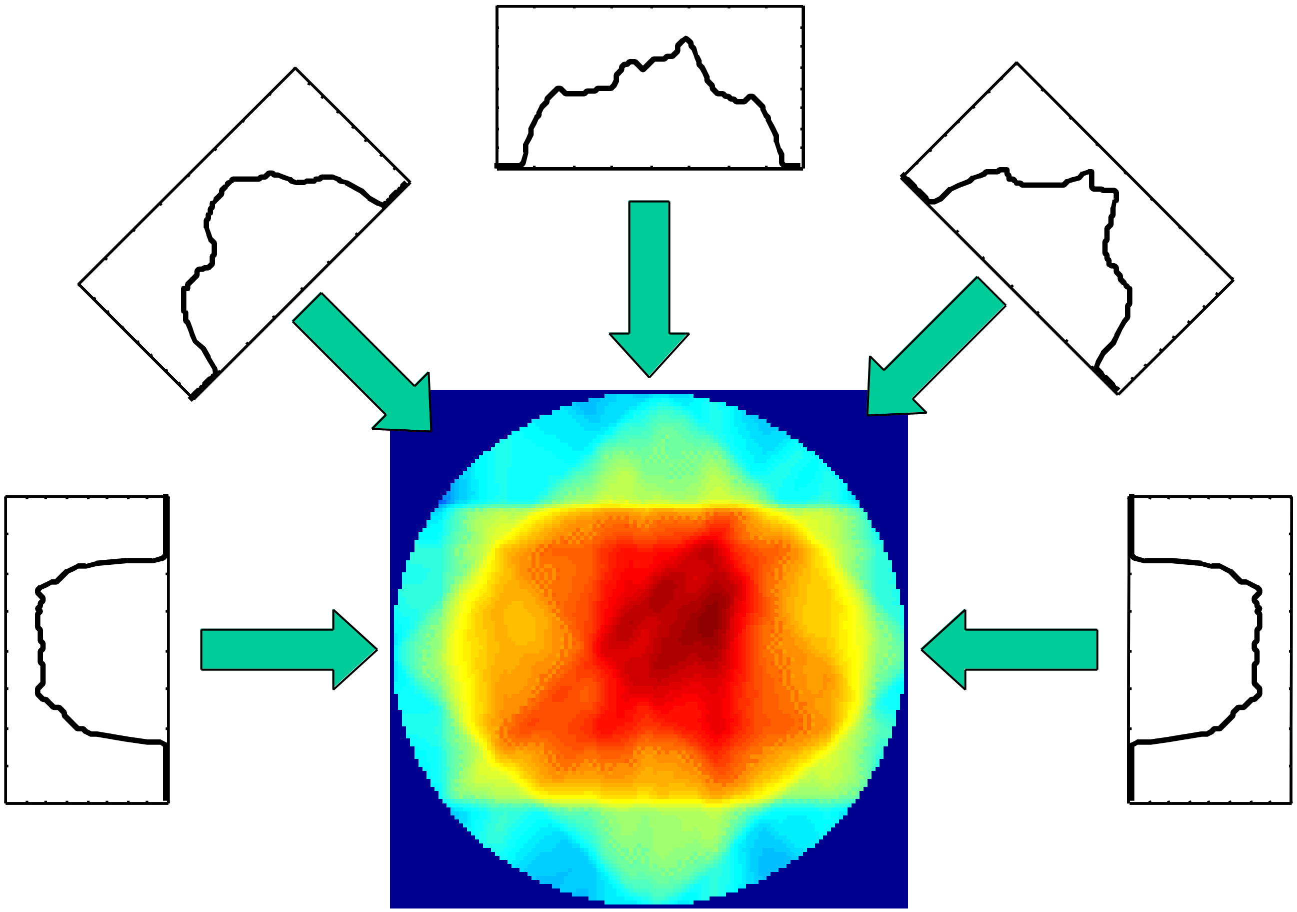

Filtered Backprojection

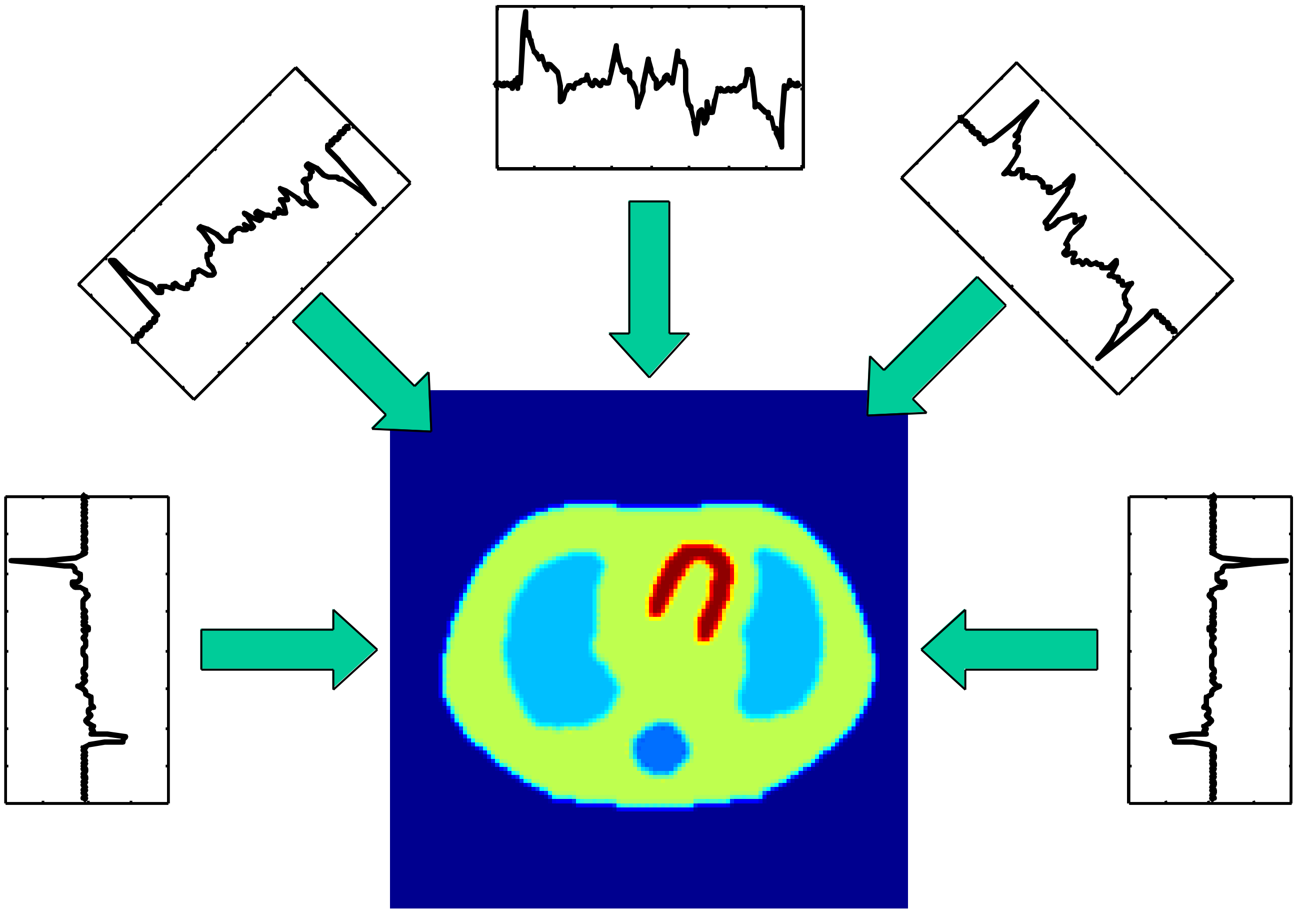

Sensitivity / Resolution Tradeoff

- **High Resolution Collimator**
  - Small position uncertainty (high resolution)
  - Collects less photons

- **High Sensitivity Collimator**
  - Collects more photons
  - Large position uncertainty (low resolution)

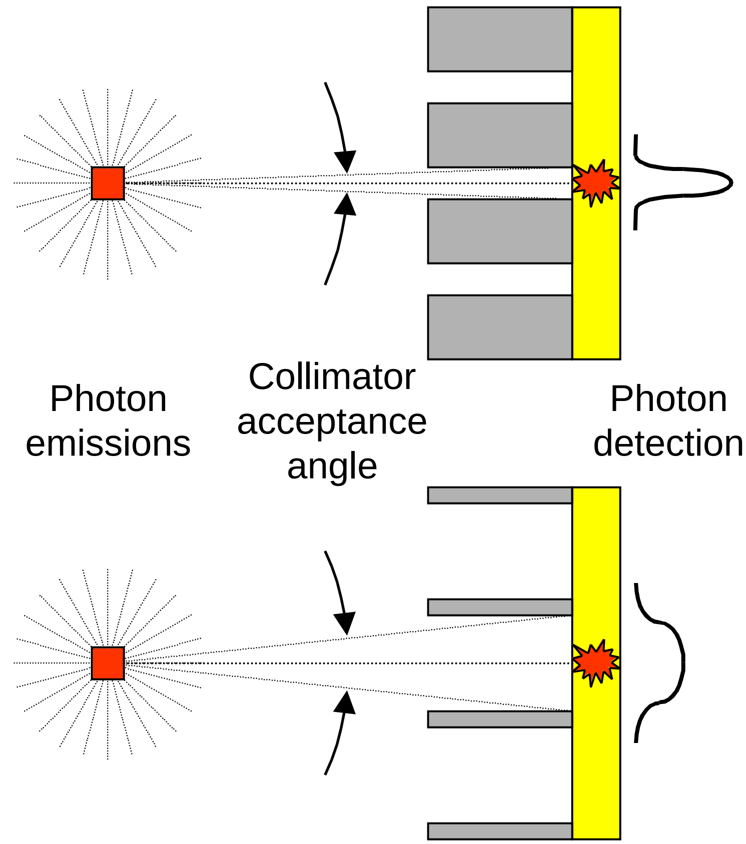

Deficiencies of Existing SPECT Systems

- **Mechanical collimators required to infer photon direction**
- **Low Sensitivity:** only small fraction (~10^{-5} or less) of total photons detected
- **Resolution Limit:** Increasing collimator size increases signal, but lose resolution
- **Dose Limitations:** Total photon flux limited by allowable radiation dose to patient
- **Septal Penetration:** Off-axis particles have significant probability of penetrating collimator at higher energies

Generic Emission Tomography Measurement Equation

$$\underline{Y} \sim Poisson\left(A\underline{\lambda} + \underline{b}\right) \text{ where}$$

- $Y_i = \#$ photons detected in the i^{th} detector bin
- $\underline{\lambda} =$ mean object intensity
- $\underline{b} =$ mean background intensity
- $A =$ system matrix $(m \times n)$ $(m \geq n)$

$$a_{ij} = P\left(\mathrm{i}^{\mathrm{th}} \text{ bin} \,\middle|\, \text{emit } \mathrm{j}^{\mathrm{th}}, \text{ Detect}\right) P\left(\text{Detect} \,\middle|\, \text{emit } \mathrm{j}^{\mathrm{th}}\right)$$

Note: $\underline{Y}$ is what we measure, but $\underline{\lambda}$ is what we want !

Statistical Image Reconstruction

- Form log-likelihood function for Poisson statistics

$$l(\underline{\lambda}) = \sum_i \left[Y_i \ln(\mu_i) - \mu_i \right] + C \quad \text{where} \quad \mu_i = \left[A\underline{\lambda} + \underline{b} \right]_i$$

- If desired, augment likelihood function with prior information on $\underline{\lambda}$ and/or roughness penalties

$$l_{pen}(\underline{\lambda}) = l(\underline{\lambda}) + p(\underline{\lambda})$$

- Solve for lambda that maximizes $l(\underline{\lambda})$

$$\hat{\underline{\lambda}} = \arg\max_{\hat{\underline{\lambda}} \geq 0} l(\underline{\lambda})$$

Linear Least-Squares Image Reconstruction

$$\hat{\underline{\lambda}}_{LS} = \left(A^T K^{-1} A\right)^{-1} A^T K^{-1} (\underline{Y} - \underline{b})$$

- Pros
  - Optimal Linear Estimator
  - Maximizes log-likelihood function $l(\underline{\lambda})$ for linear additive Gaussian measurement statistics (or high count-rate Poisson statistics)
  - Non-iterative direct solution
- Cons
  - Requires solving large # of simultaneous equations
  - Ill-conditioned
  - $\hat{\underline{\lambda}}_{LS}$ may have negative values (!)
  - Difficult to incorporate roughness penalties

Iterative Image Reconstruction: The EM Algorithm

$$\hat{\lambda}_j^{k+1} = \frac{\hat{\lambda}_j^k}{s_j} \sum_i \frac{a_{ij} Y_i}{\sum_l a_{il} \hat{\lambda}_l^k} \quad \text{where} \quad s_j \equiv \sum_i a_{ij}$$

- Pros
  - Maximizes log-likelihood function $l(\underline{\lambda})$ for Poisson statistics
  - Non-negativity constraints “built-in”
  - Can easily incorporate roughness penalty functions
- Cons
  - Iterative (when do you stop iterating?)
  - Slow to converge (what is convergence criteria?)

Roughness Penalty

- Adding a quadratic roughness penalty to log-likelihood function biases estimate $\hat{\underline{\lambda}}$ towards "smoother" images

$$p(\underline{\lambda}) = -\tfrac{1}{2}\beta \sum_{i,j=1}^{N} W_{ij}(\lambda_j - \lambda_i)^2$$

$$\text{where } W_{ij} = \begin{cases} 1 & (i,j) \text{ neighbors} \\ 0 & \text{otherwise} \end{cases}$$

First-Order Neighborhood (North, South, East, West)

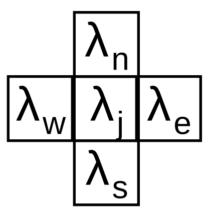

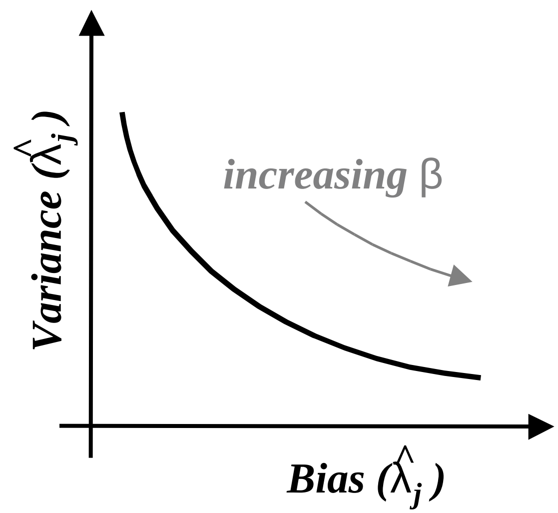

Example: EM Algorithm with Roughness Penalty

10^6 counts, 100 iterations

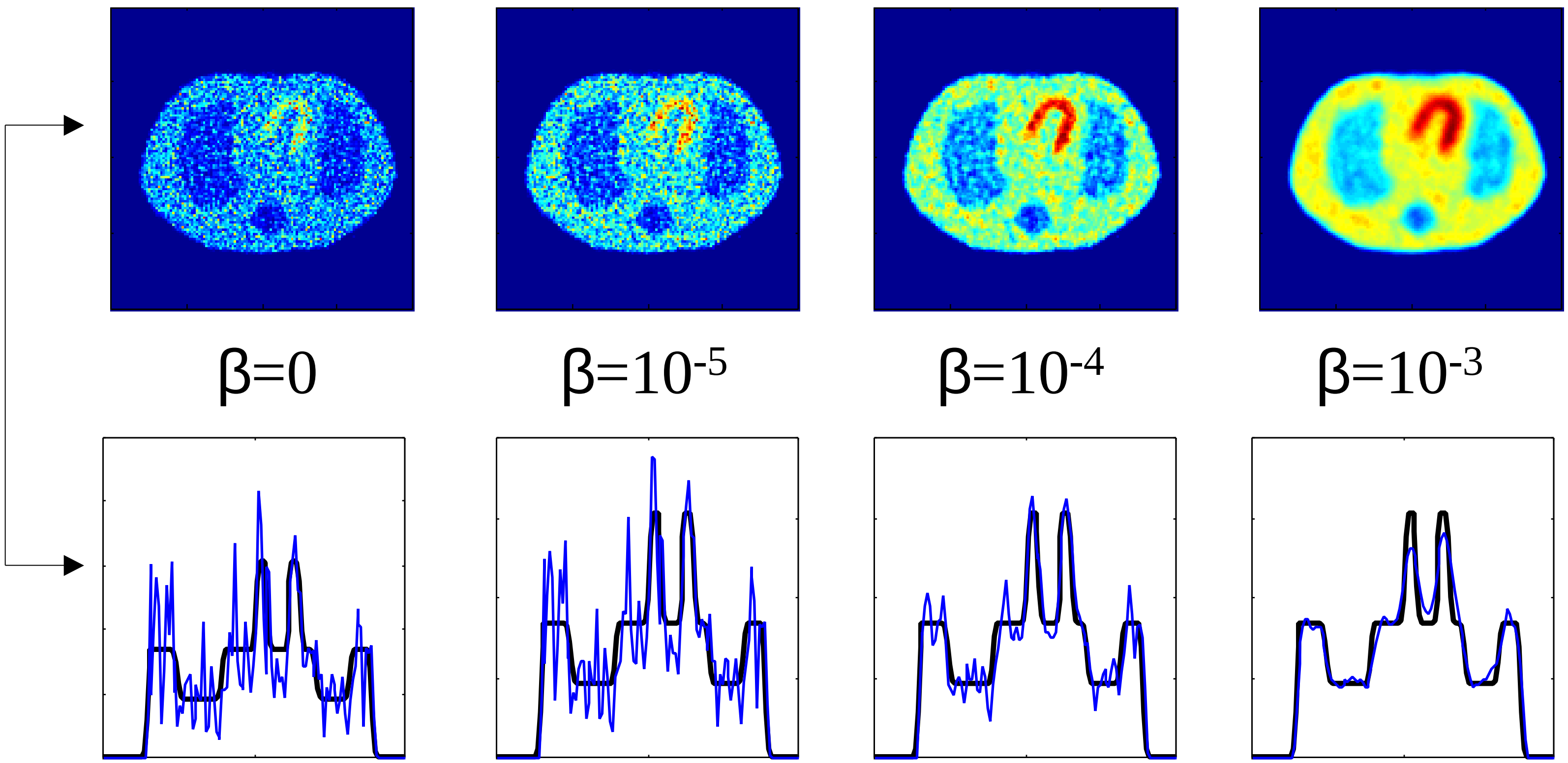

Compton Scatter Angle / Energy Relationship (Simple Model)

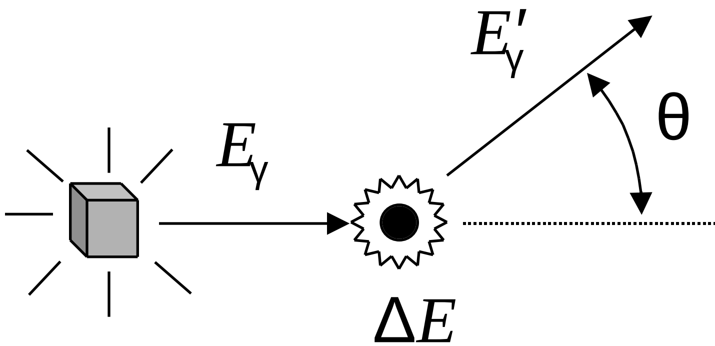

$$\Delta E = E_\gamma \left[1 - \frac{1}{1 + \left(\frac{E_\gamma}{511} \right) (1 - \cos\theta)} \right]$$

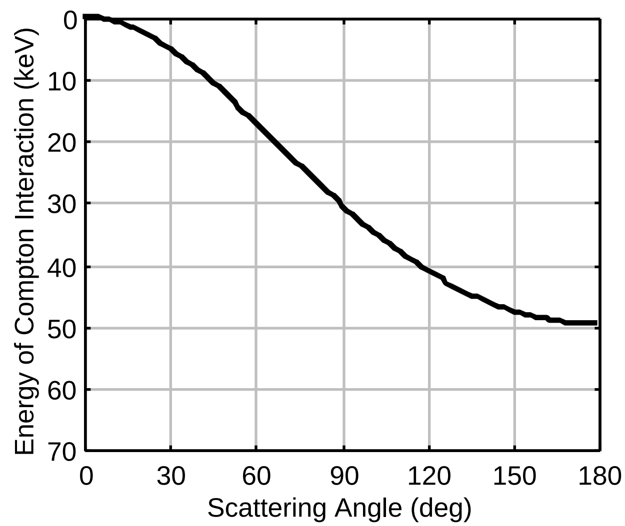

Compton Scatter Angle / Energy Relationship (Detailed Model)

Electron at rest

$$E'_\gamma = \frac{E_\gamma}{1 + \frac{E_\gamma}{m_0 c^2}\left(1 - \cos\theta\right)}$$

Electron in motion

$$p_z c = -(m_0 c^2)\frac{\left(1 - \frac{E'_\gamma}{E_\gamma}\right) - \frac{E'_\gamma}{m_0 c^2}\left(1 - \cos\theta\right)}{\sqrt{1 + \left(\frac{E'_\gamma}{E_\gamma}\right)^2 - 2\left(\frac{E'_\gamma}{E_\gamma}\right)\cos\theta}}$$

Doubly differential cross section

$$f(\theta, E'_\gamma) = \frac{\pi r_0^2 \sin\theta}{E_\gamma}\left(\frac{E'_\gamma}{E_\gamma} + \frac{E_\gamma}{E'_\gamma} - \sin^2\theta\right)\frac{p_z J_n(p_z)}{1 - \frac{E'_\gamma}{E_\gamma} + \frac{E_\gamma}{m_0 c^2}(1 - \cos\theta)}$$

Compton profiles

Compton Scatter Angle / Energy Relationship (Detailed Model)

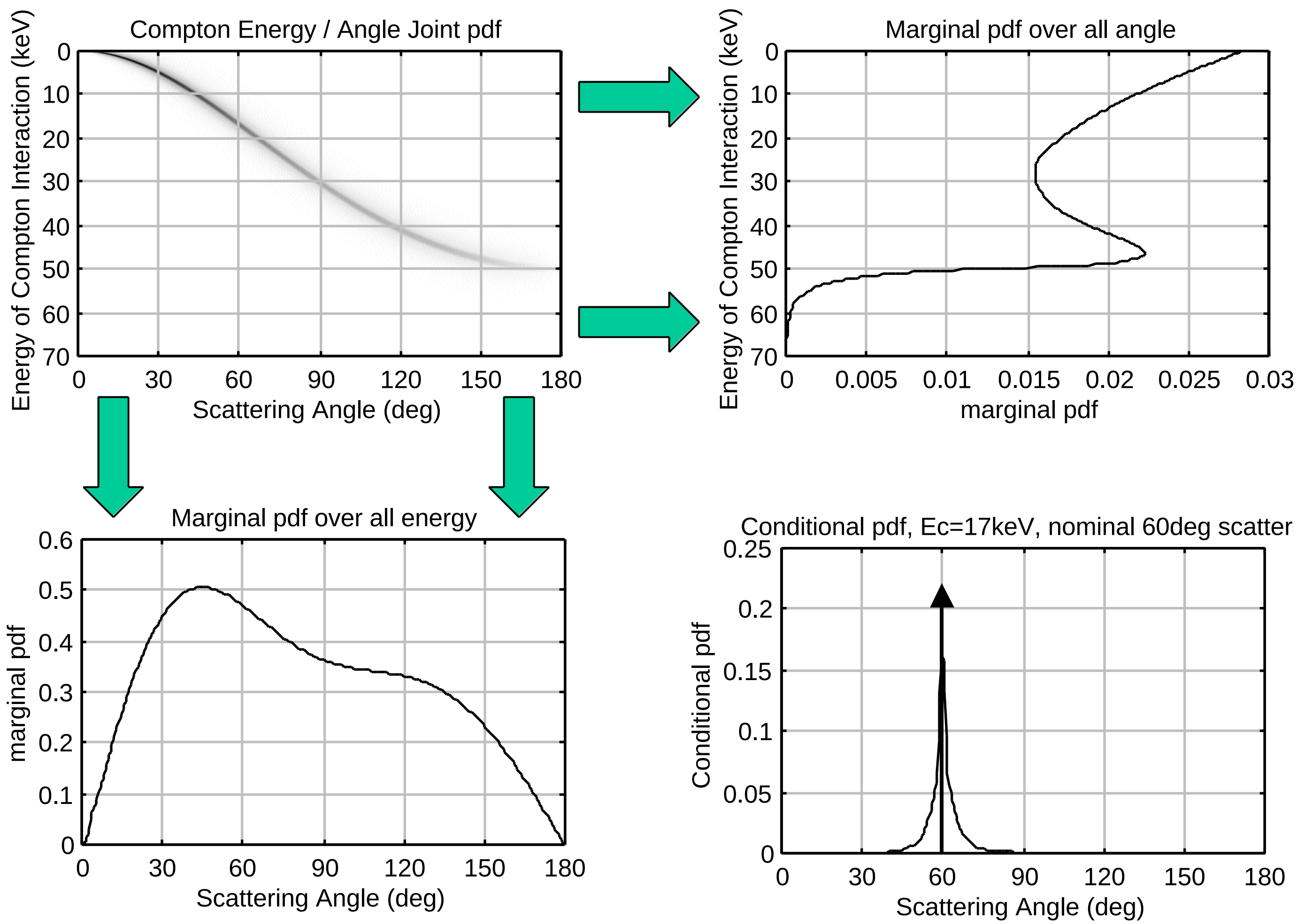

Compton-SPECT Camera Operating Principles

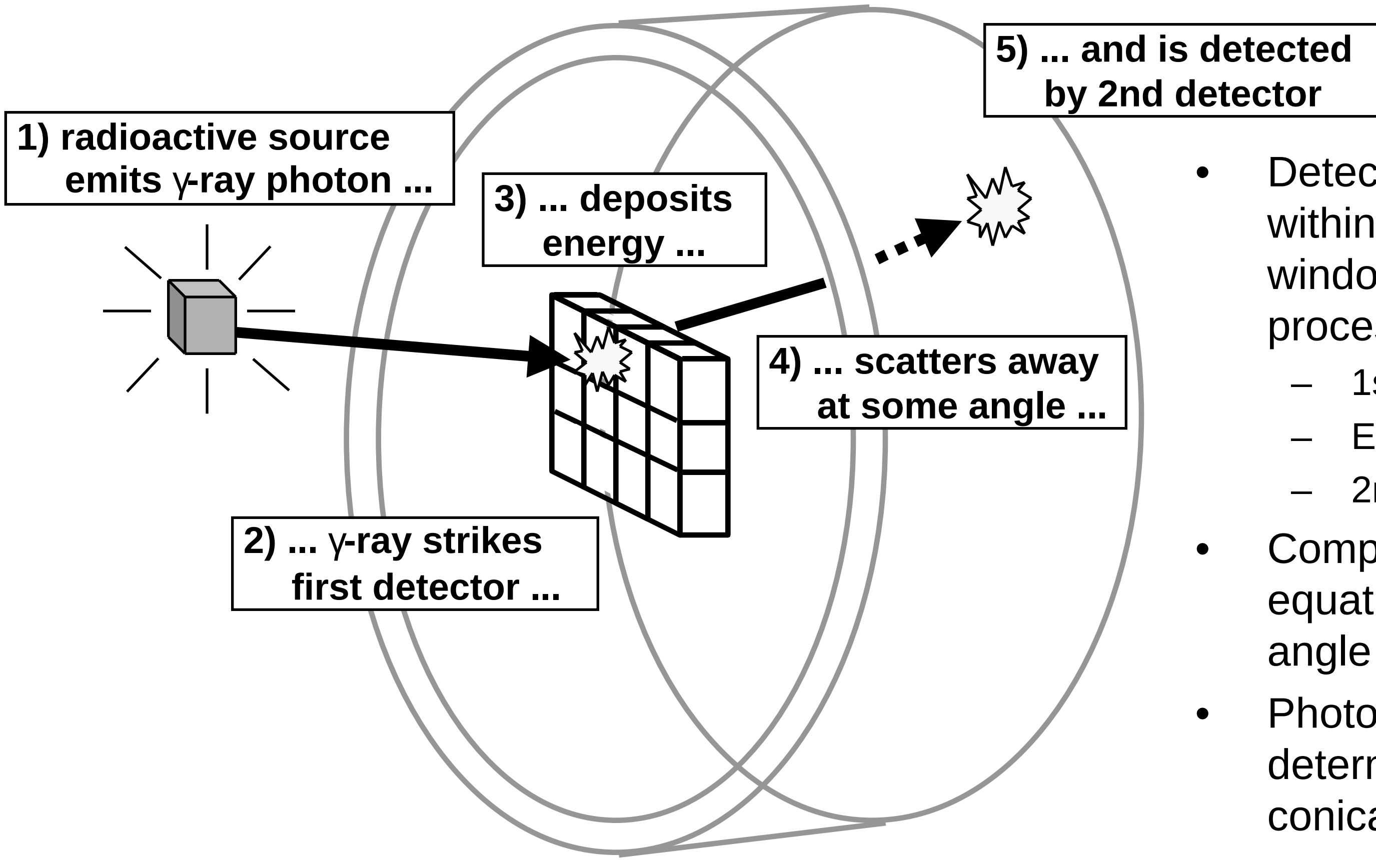

- Detections occurring within a small time window are recorded for processing
  - 1st Detector Position
  - Energy Deposited
  - 2nd Detector Position
- Compton scatter equation relates scatter angle / energy
- Photon direction determined to within a conical ambiguity

Single Measurement Backprojection Cone

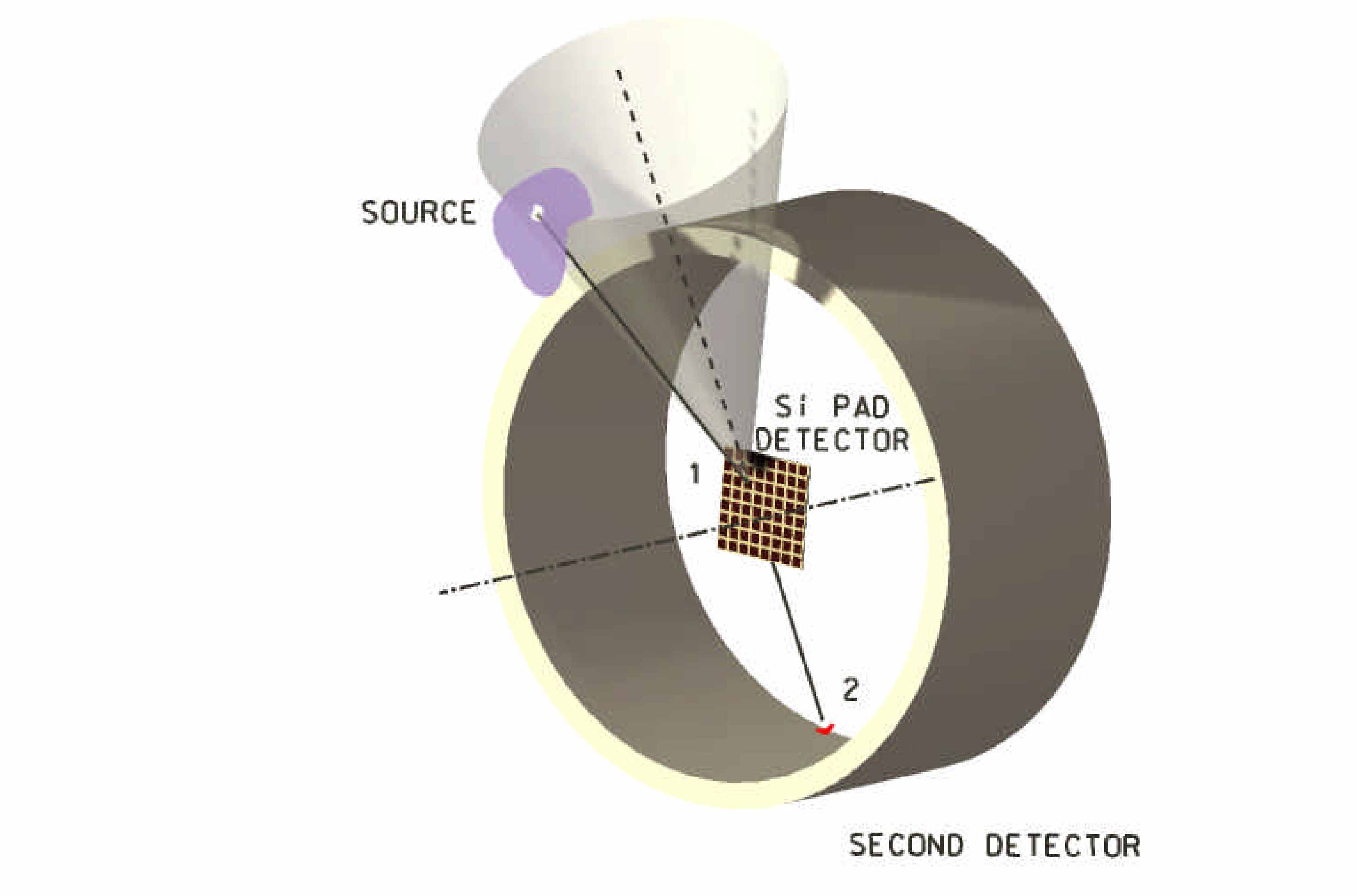

Multiple Measurements Intersecting at Source Location

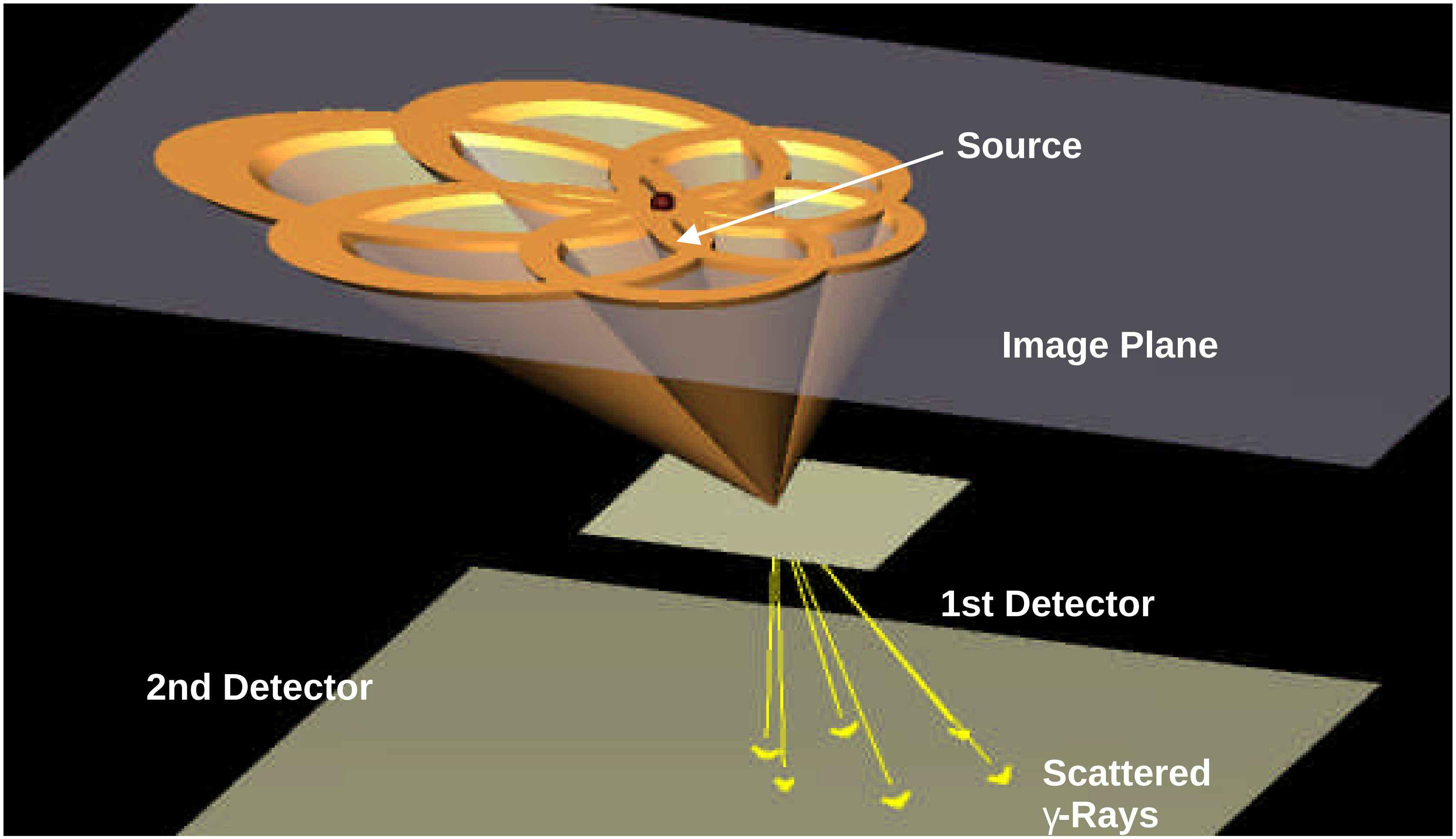

University of Michigan Compton-SPECT System

- Silicon 1st-Detector
  - 4.5cm x 1.4cm x 0.03cm
- NaI 2nd Detector
  - 50cm diameter
  - 10cm deep
  - 11 detector modules, arranged around circumference

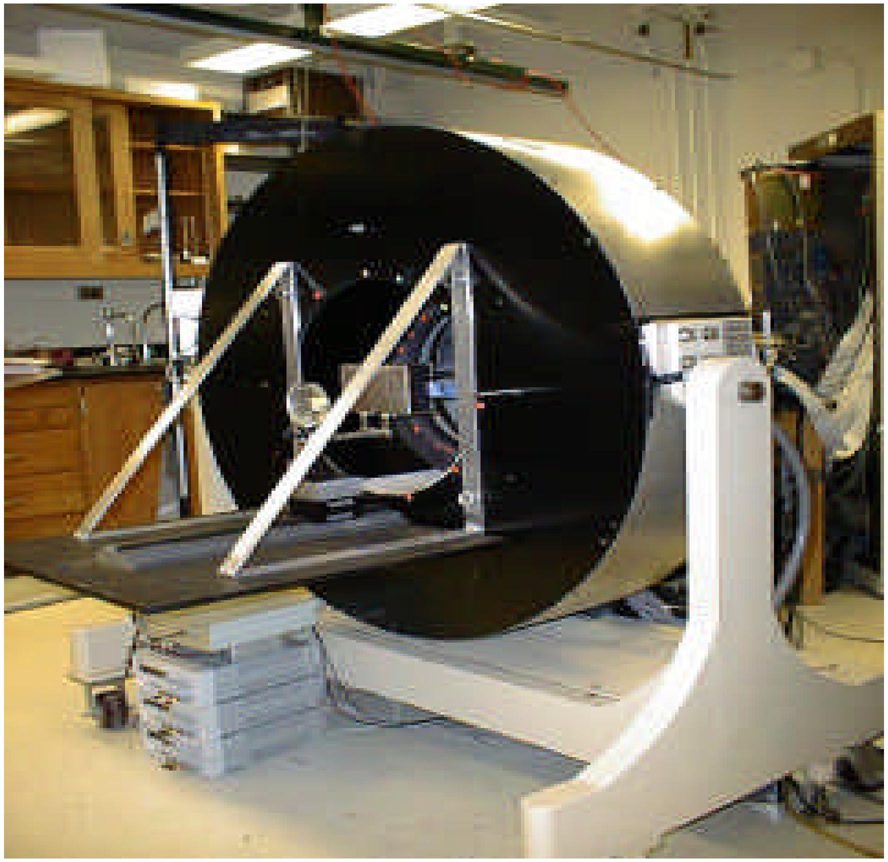

Silicon Pad Detector Unit
(1st Detector)

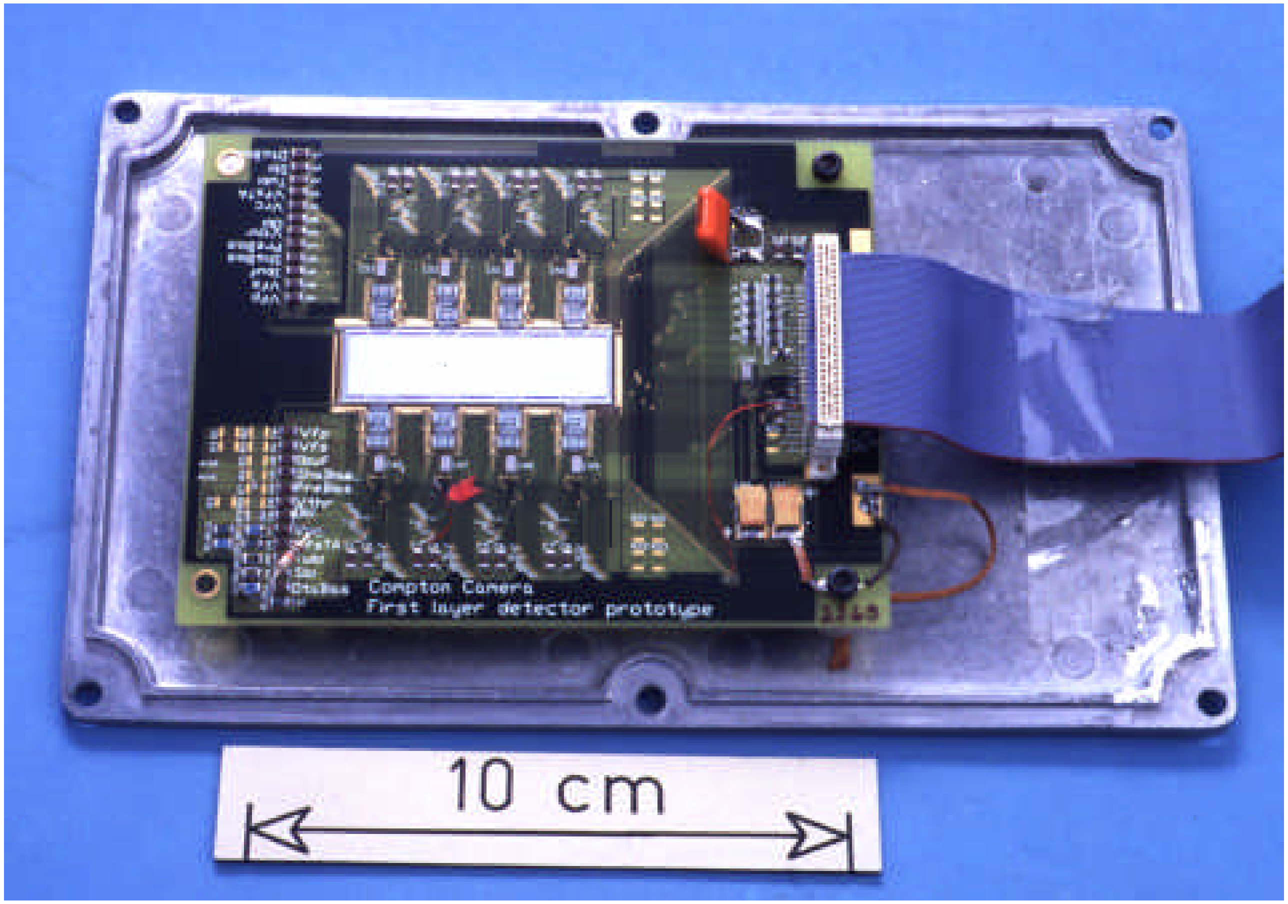

Silicon Pad Detector (1st Detector)

- 300 μm thick and rectangular (4.5 cm × 1.4 cm)
- 32×8 (256) pads, pixel size 1400 μm, fully depleted at 60 V

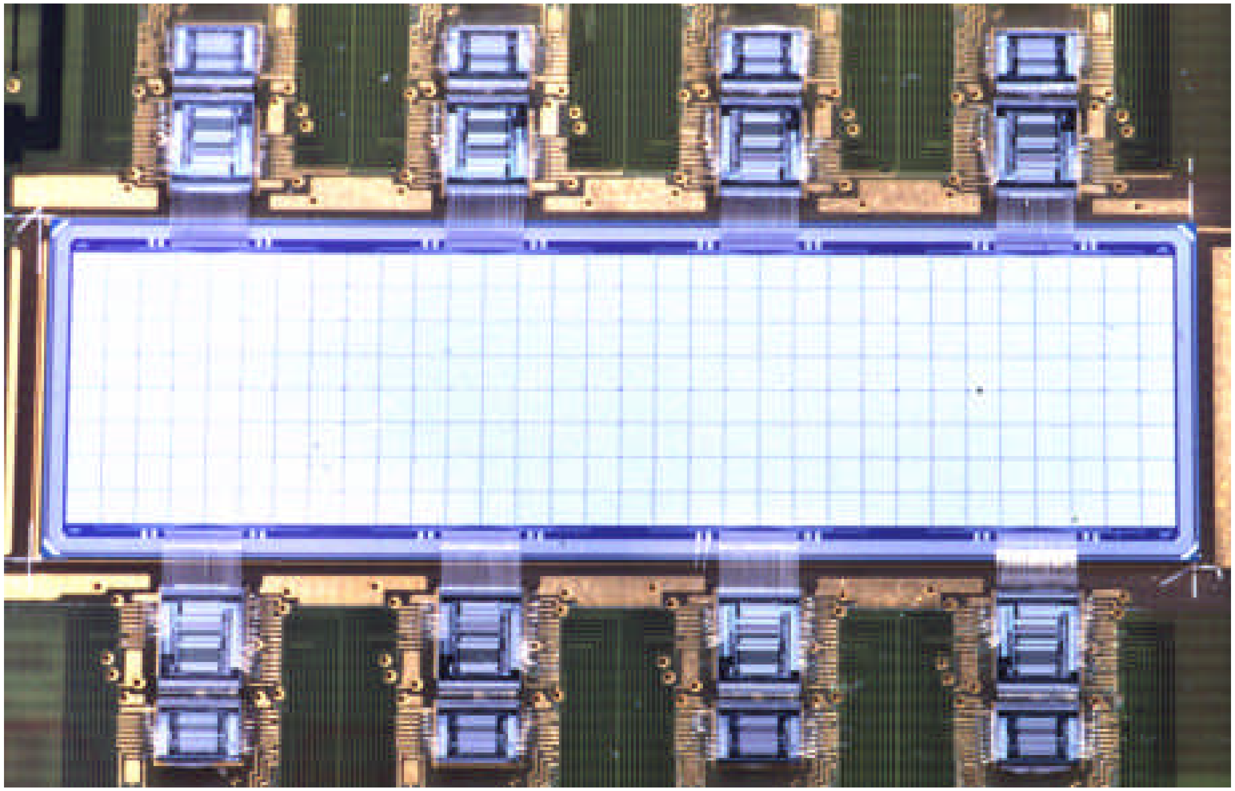

Sodium Iodide Scintillater Module (2nd Detector)

- Ring detectors consists of 11 NaI scintillation detector modules arranged around a 50cm diameter, 10cm long cylinder.
- Each module is composed of a 15cm array of 1.27cm thick and 3mm wide NaI bars viewed by 20 photo-multiplier tubes.
- Intrinsic spatial resolution is 3 mm FWHM. Energy resolution is 18keV FWHM (13%) at 140 keV.

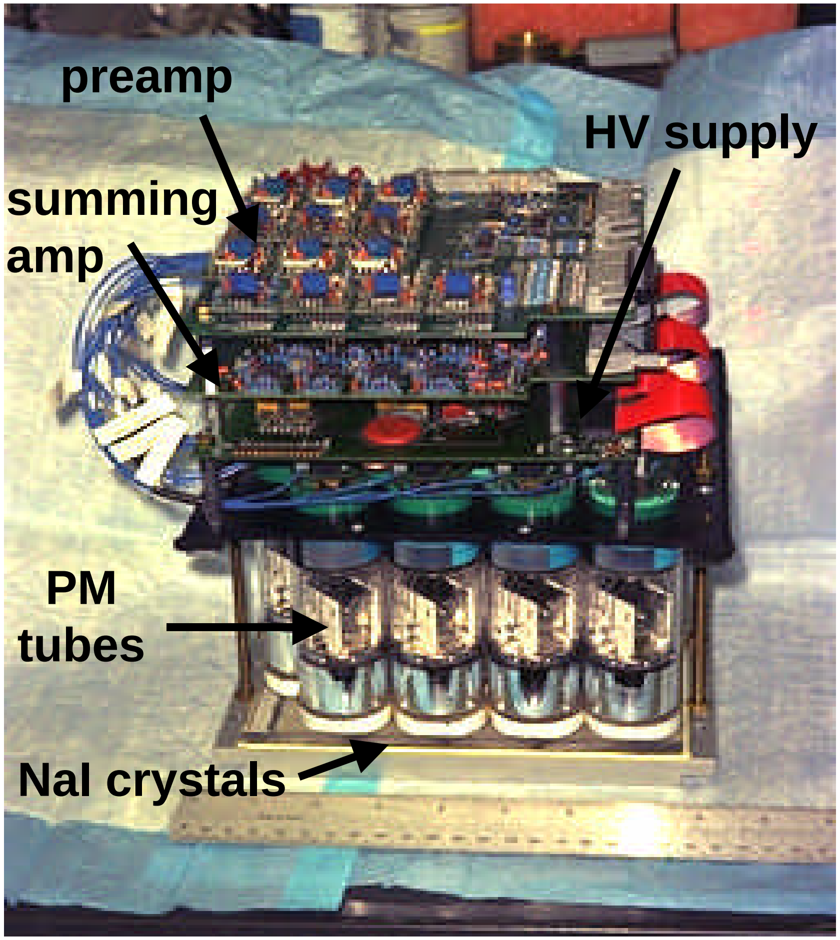

Compton-SPECT System Block Diagram

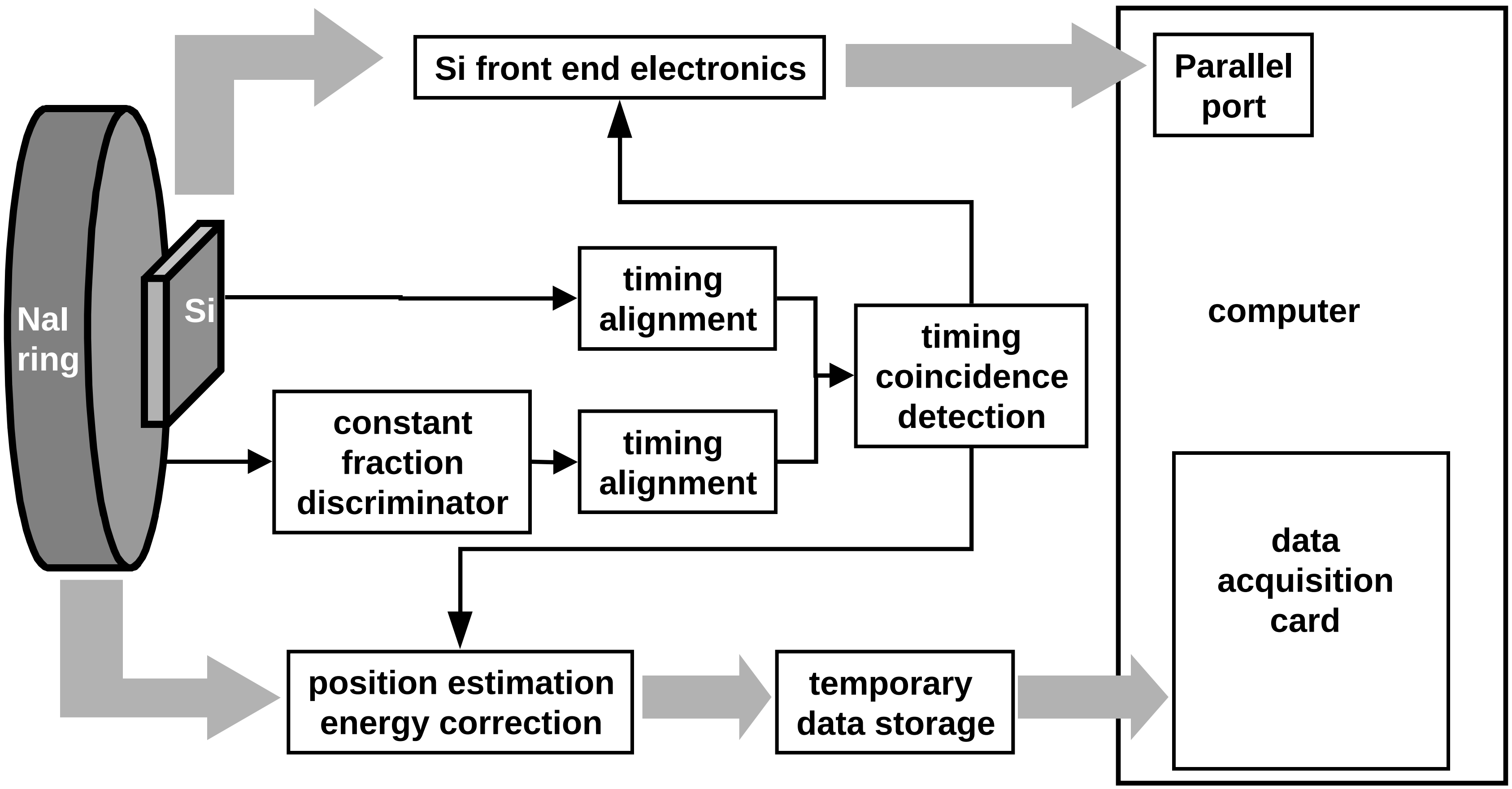

What do we end up measuring?

- Measure various attributes of ***each*** photon detection
  - Position
  - Energy deposited
- Photon measurements are stored in a sequential list

Detector #1 Detector #2

Photon 1 -- E1, X1, Y1, Z1, E2, X2, Y2, Z2
Photon 2 -- E1, X1, Y1, Z1, E2, X2, Y2, Z2
⋮
Photon M -- E1, X1, Y1, Z1, E2, X2, Y2, Z2

What do we do with all that data?

- HUGE system matrix for C-SPECT if we calculate probabilities a_{ij} for every possible measurement
  – Example: simple 2D reconstruction
    - Source Plane Pixels 64^2
    - 1st Detector Pixels 1 (point detector)
    - 2nd Detector Pixels 512 x 128 (3mm x 3mm square)
    - Matrix Size 2^{28} elements (256 megabytes)
  – Add a few more parameters...
    - 3D Source Pixels 64 additional source planes
    - 1st Detector Pixels 32 x 8 array
    - Energy Channels 64 (~750eV resolution)
    - Matrix Size 2^{48} elements (petabyte range...)

Cutting down the Computations

- Not all measurement bins contain measurements
  - Typically collect 10^5 to 10^7 counts (photon measurements)
  - Even for simple Compton-SPECT example,
    number of bins = $2^{28} \approx 10^{8.4}$ >> number of counts

- What happens when bin-size becomes infinitesimal?
  - Continuous measurements
  - Each measurement is of a single photon
  - Calculate probability of a single photon measurement
  - Listmode Likelihood

Listmode EM

- From before

$$a_{ij} = P\left(\mathrm{i^{th}\text{ - bin}} \,\middle|\, \mathrm{Detect,\ emit\ j^{th}} \right) P\left(\mathrm{Detect} \,\middle|\, \mathrm{emit\ j^{th}} \right)$$

- We now treat each measurement in the list as its own "bin", containing a single photon measurement $\underline{\mathrm{A}}_{\mathrm{i}}$

$$\underline{\mathrm{A}}_{\mathrm{i}} = \left[e_1, x_1, y_1, z_1, e_2, x_2, y_2, z_2 \right]_i \quad \text{with associated density}$$

$$p\left(\underline{\mathrm{A}}_{\mathrm{i}} \,\middle|\, \mathrm{Detect,\ emit\ j^{th}} \right) P\left(\mathrm{Detect} \,\middle|\, \mathrm{emit\ j^{th}} \right)$$

Model Approximations

- Dominant factors include:
  - Doppler Broadening
  - Energy Measurement Error

- Approximations & Assumptions:
  - Perfect position resolution (δ-function)
  - Gaussian energy measurement error

- Results in tractable expressions for $f\left(\theta, E'_\gamma\right)$ and a_{ij} which can be pre-computed and stored.

^{99m}Tc and ^{131}I Point Source Images (2D)

Single on-axis point source at 10 cm

100K coincident events

100K coincident events

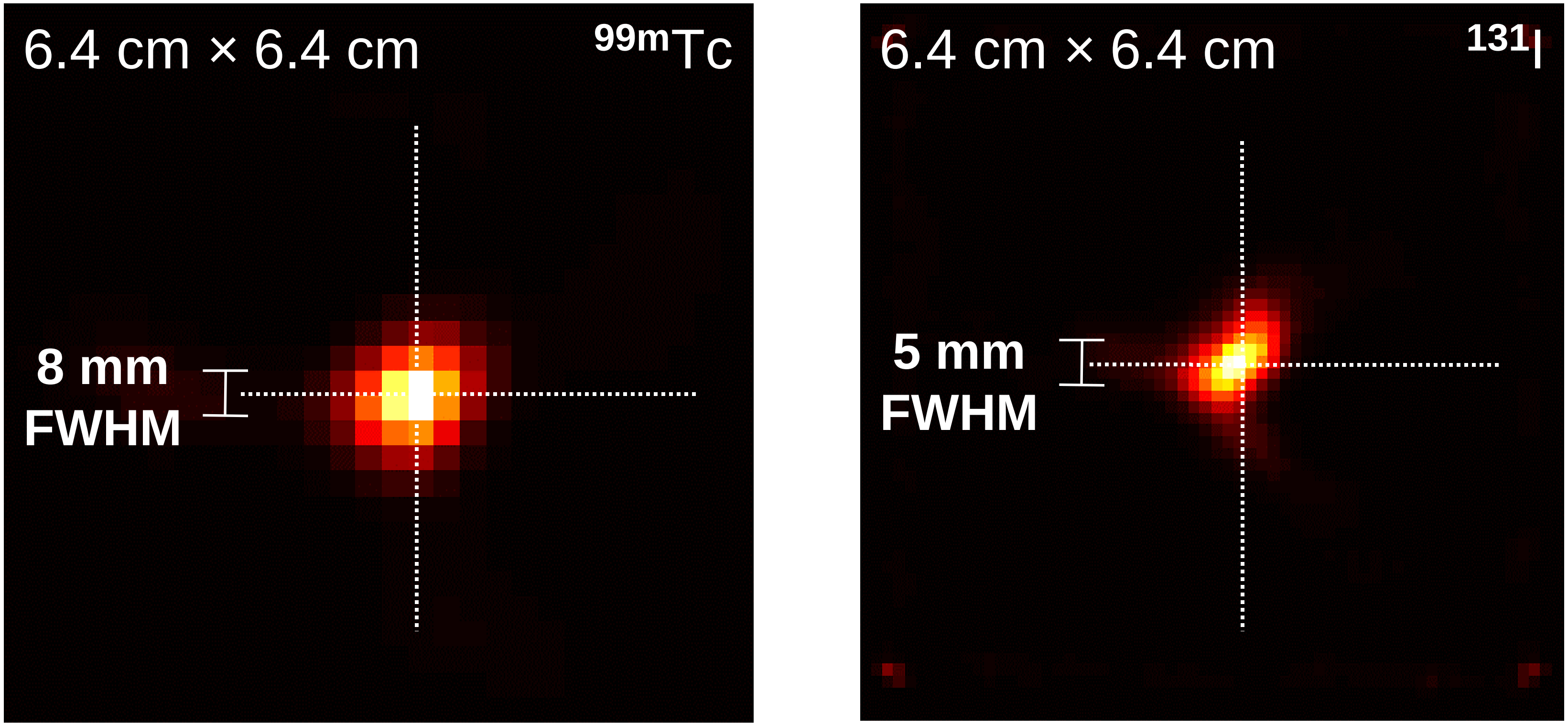

^{99m}Tc Line Source Image (2D)

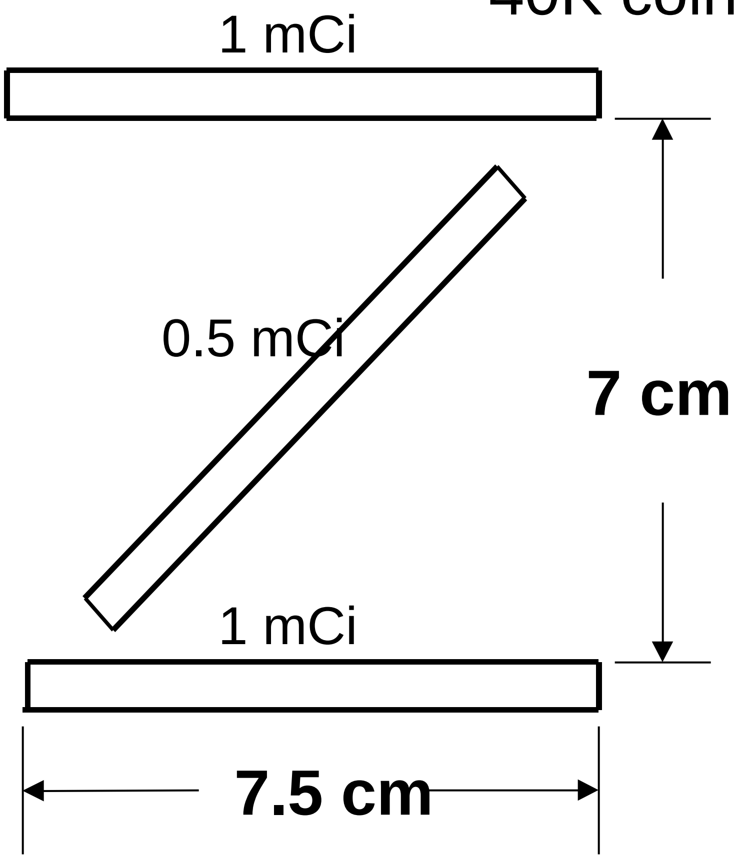

40K coincident events

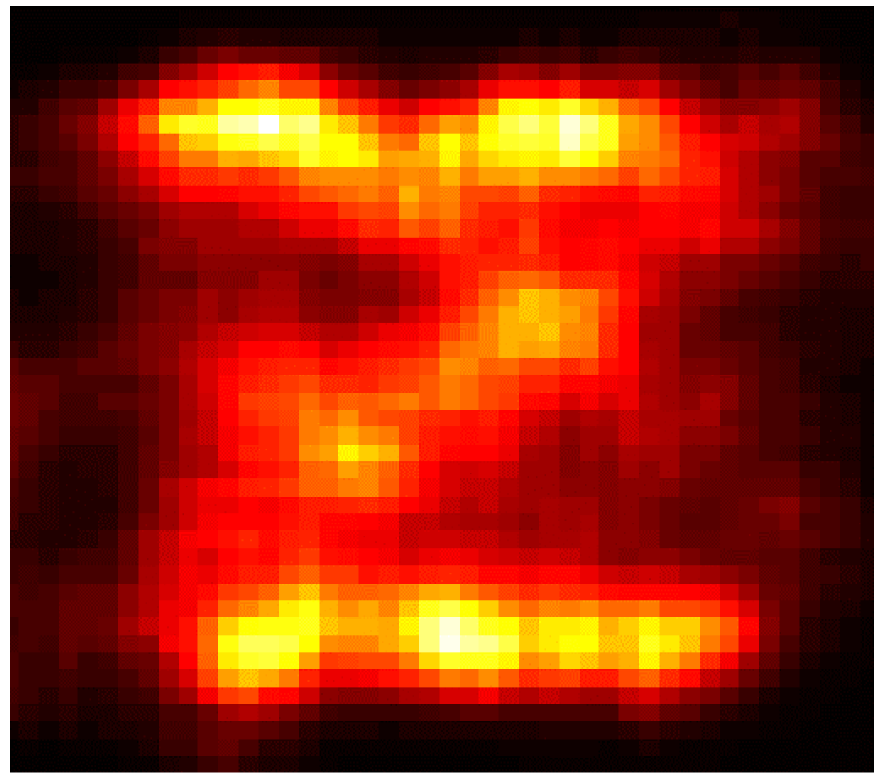

Hot Spot on Warm Background (^{131}I, 2D)

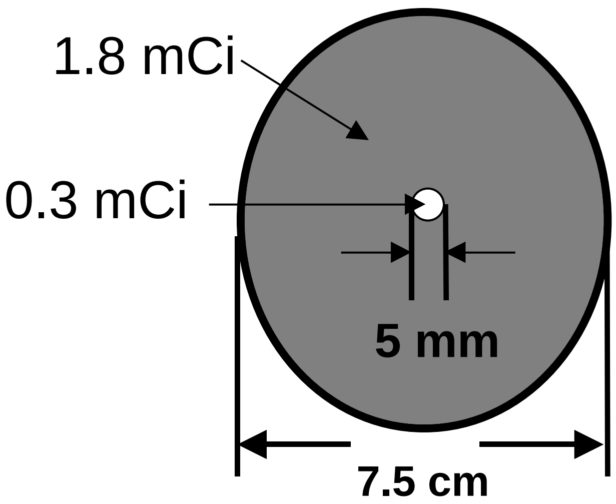

70K coincident events

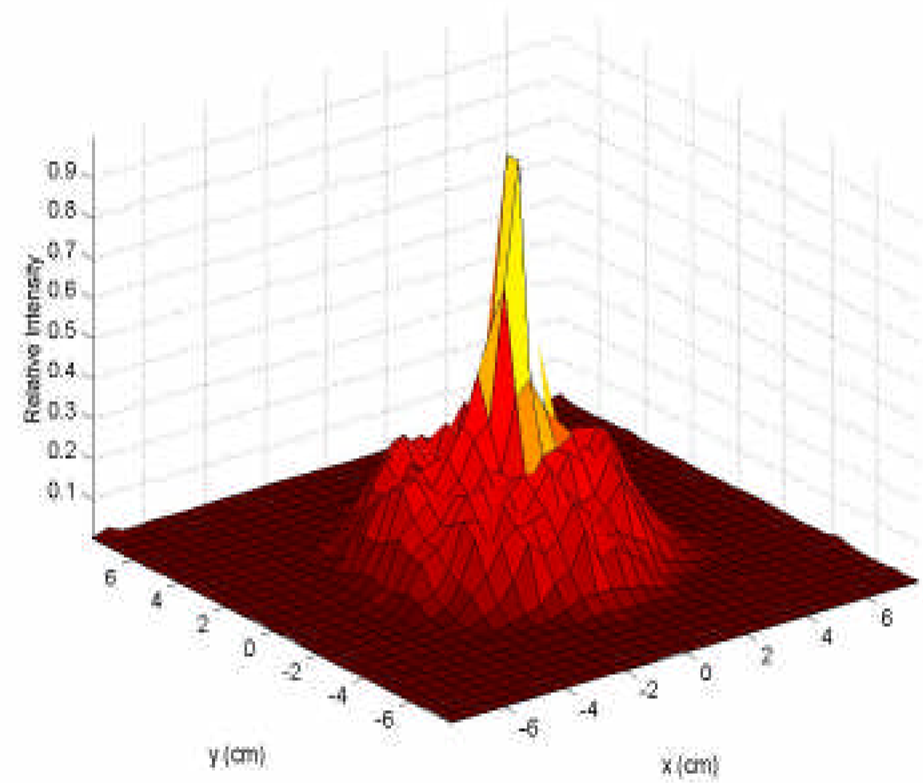

Hot Spots placed on Uniform Disk Background (99mTc, 2D)

- Ordered-Subsets EM
  - 4 iterations @ 10subsets / iteration
- No smoothing penalty
- 77k counts

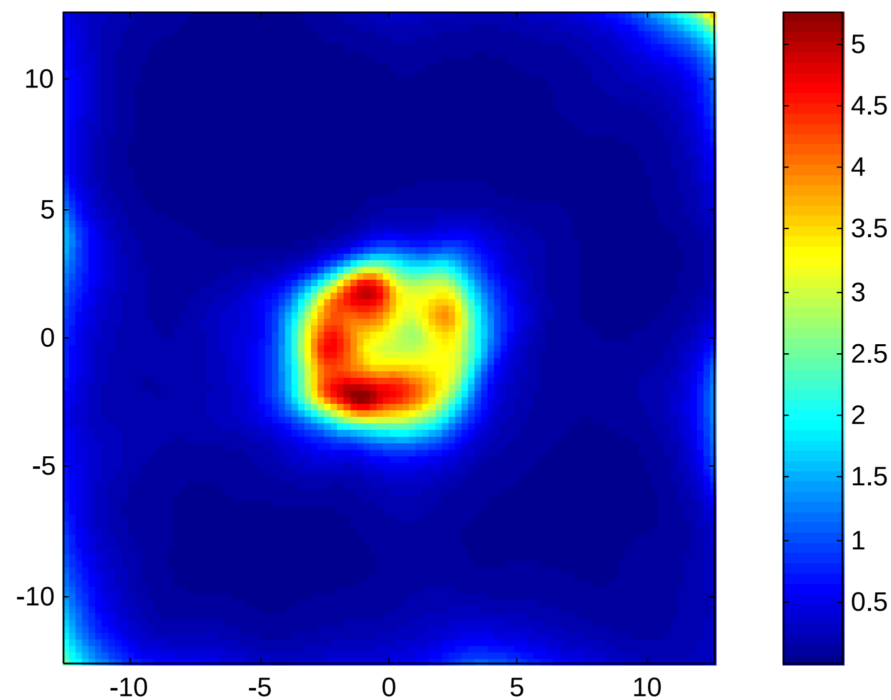

Feasibility Analysis

- Question: Can we get as good or better C-SPECT images as with SPECT?
- Can test performance by:
  - Constructing Prototype (…or…)
  - Performing Extensive Simulations (…or…)
  - Establish tight lower bounds on achievable accuracy of reconstructed images
- Criteria:
  - Bias $b_\theta\left(\hat{\theta}_1\right) = E_\theta\left[\hat{\theta}_1 - \theta\right]$
  - Variance $\mathrm{var}_\theta\left(\hat{\theta}_1\right) = E_\theta\left[\left(\hat{\theta}_1 - E_\theta\left(\hat{\theta}_1\right)\right)^2\right]$
  - Mean Square Error $MSE_\theta\left(\hat{\theta}_1\right) = \mathrm{var}_\theta\left(\hat{\theta}_1\right) + b_\theta^{\,2}\left(\hat{\theta}_1\right)$

Unbiased Cramer-Rao Bound

$$\mathrm{var}_{\underline{\theta}}\left(\hat{\underline{\theta}}\right) \geq F_{\underline{\theta}}^{-1} \text{ for any unbiased estimator } \hat{\underline{\theta}}(y)$$

$$F_{\underline{\theta}} = E_{\underline{\theta}}\left[- \quad {}^{2} l(\underline{\theta})\right] \text{ is the Fisher Information Matrix}$$

$$l(\underline{\theta}) \text{ is the log-likelihood function}$$

- Difficulty: Image reconstruction is usually ***biased*** due to finite resolution limits

Biased Cramer-Rao Bound

$$\mathrm{var}_{\underline{\theta}}\left(\hat{\theta}_j\right) \geq \left[e_j + {}_{\underline{\theta}} b_{\underline{\theta}}\left(\hat{\theta}_j\right)\right]^T F_{\underline{\theta}}^{-1}\left[e_j + {}_{\underline{\theta}} b_{\underline{\theta}}\left(\hat{\theta}_j\right)\right]$$

for any estimator $\hat{\underline{\theta}}$ with bias $b_{\underline{\theta}}$

- Difficulty: This bound is only useful for comparing between estimators with ***identical bias gradients*** ${}_{\underline{\theta}} b_{\underline{\theta}}$

Uniform Cramer-Rao Bound

$$\operatorname{var}_{\underline{\theta}}\left(\hat{\theta}_j\right) \geq \left[e_j + \underline{d}_{\min}(\underline{\theta})\right]^T F_{\underline{\theta}}^{-1}\left[e_j + \underline{d}_{\min}(\underline{\theta})\right]$$

for any estimator $\underline{\hat{\theta}}$ with bias gradient length $\left\| \quad {}_{\underline{\theta}} b_{\underline{\theta}}\left(\hat{\theta}_j\right) \right\|$

satisfying $\left\| \quad {}_{\underline{\theta}} b_{\underline{\theta}}\left(\hat{\theta}_j\right) \right\| \leq \delta$

- Issue: Achievability

Example Uniform Cramer-Rao Bound Curve

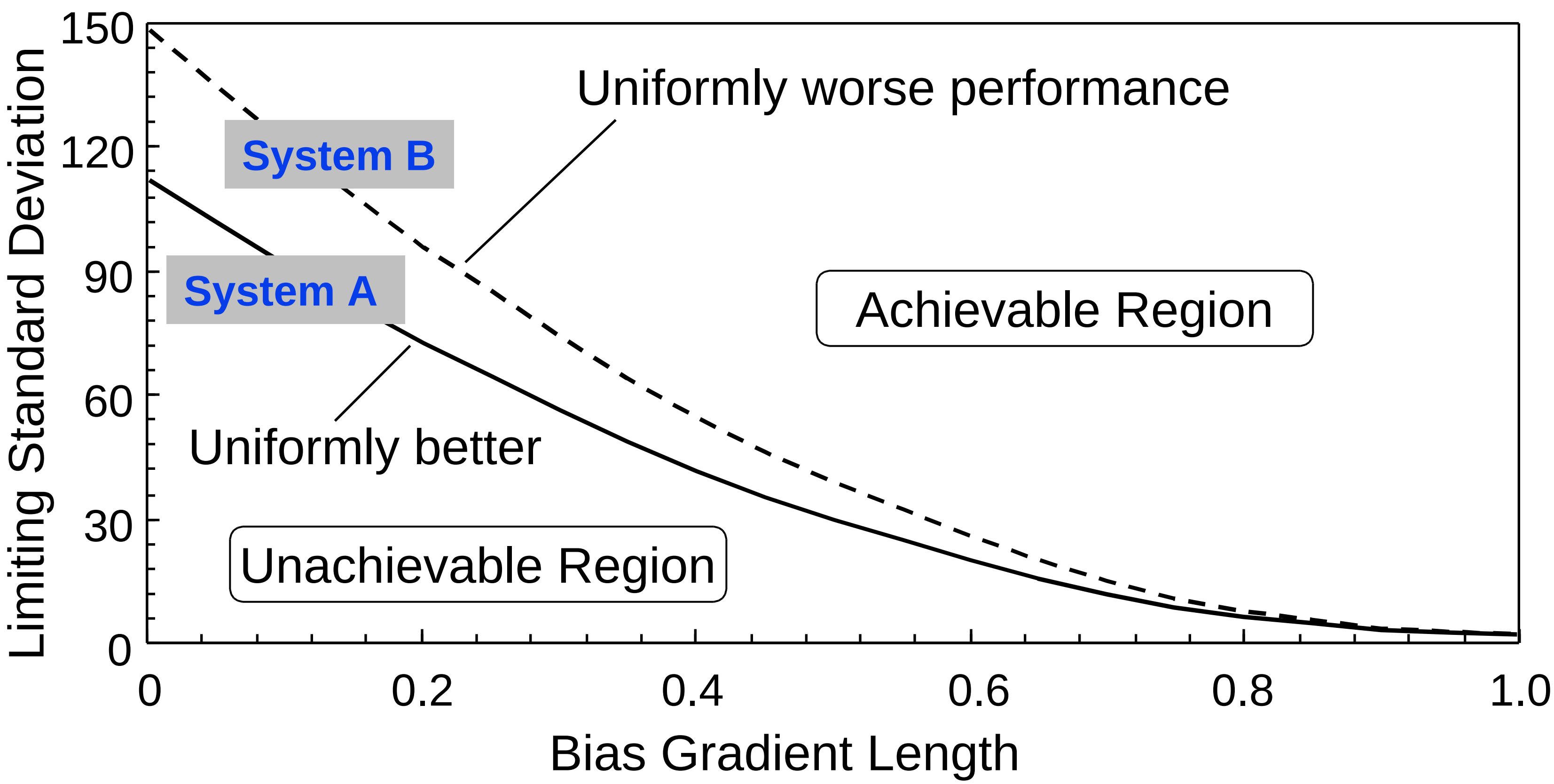

Achievability of UCRB

For $\underline{\theta}$ = source intensity vector $\underline{\lambda}$,

UCRB is nearly attainable by the

Penalized Maximum Likelihood estimator

$$\hat{\underline{\theta}} = \arg\max_{\hat{\underline{\theta}} \geq 0} \left\{ l(\underline{\theta}) + \beta \underline{\theta}^T P \underline{\theta} \right\}$$

- Issue: What is the meaning of bias gradient constraint?

UCRB Calculation

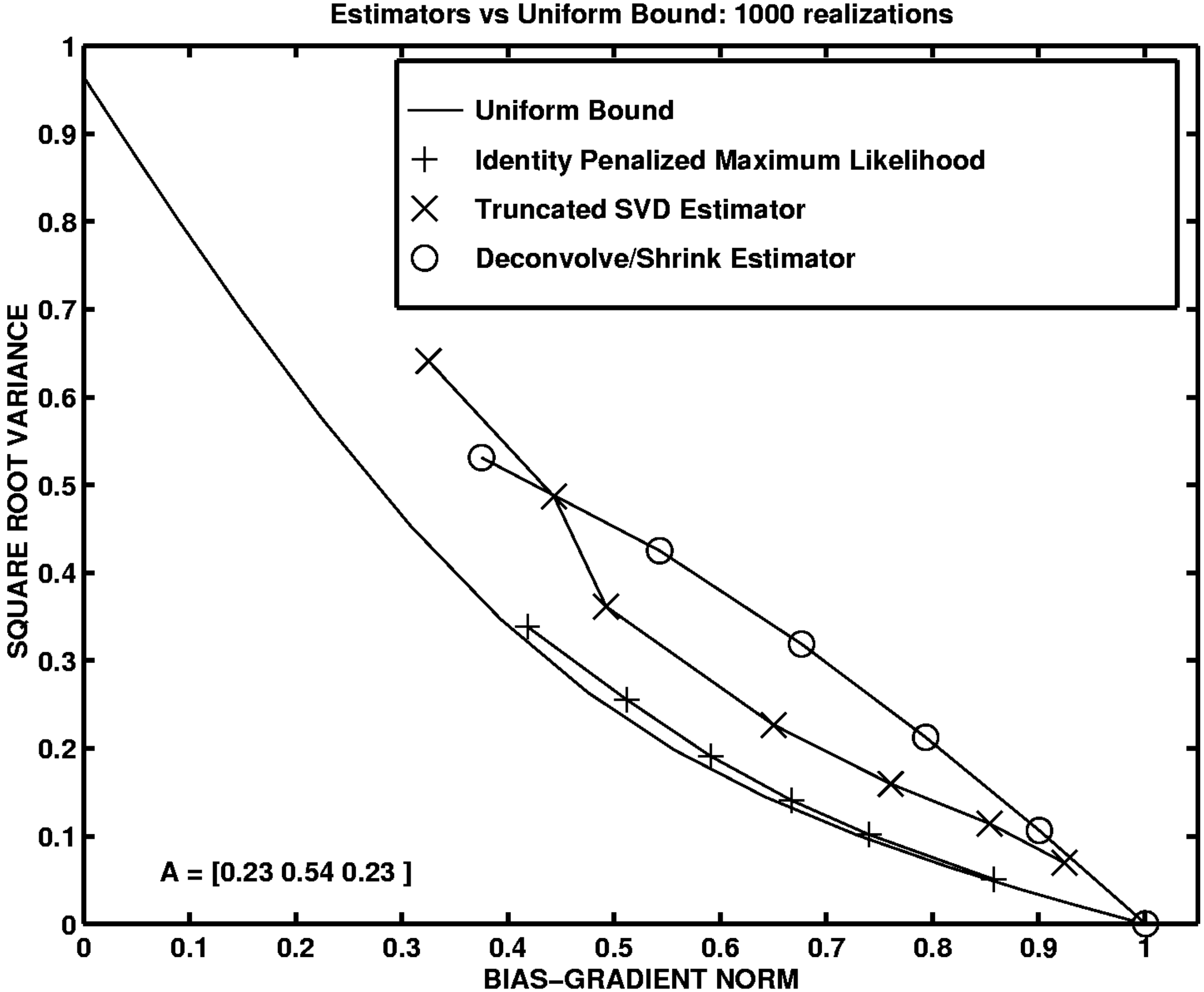

Bias Gradient Approximates Recoverable Resolution

For the PML Estimator,

$$b_{\underline{\theta}}\left(\hat{\theta}_j\right) = F_{\underline{\theta}}\left[F_{\underline{\theta}} + \beta P\right]^{-1} e_j - e_j + O\left(1/\beta^2\right) \quad \text{so that}$$

$$\left\| b_{\underline{\theta}}\left(\hat{\theta}_j\right) \right\| = \left\| E_{\underline{\theta}=e_j}\left[\hat{\underline{\theta}}\right] - e_j \right\| + O\left(1/\beta^2\right) \quad \text{when P and } F_{\underline{\theta}} \text{ commute}$$

Estimation Performance Comparison with ^{99m}Tc

- Same counts, estimate center pixel of a 7.5cm diameter uniform disk

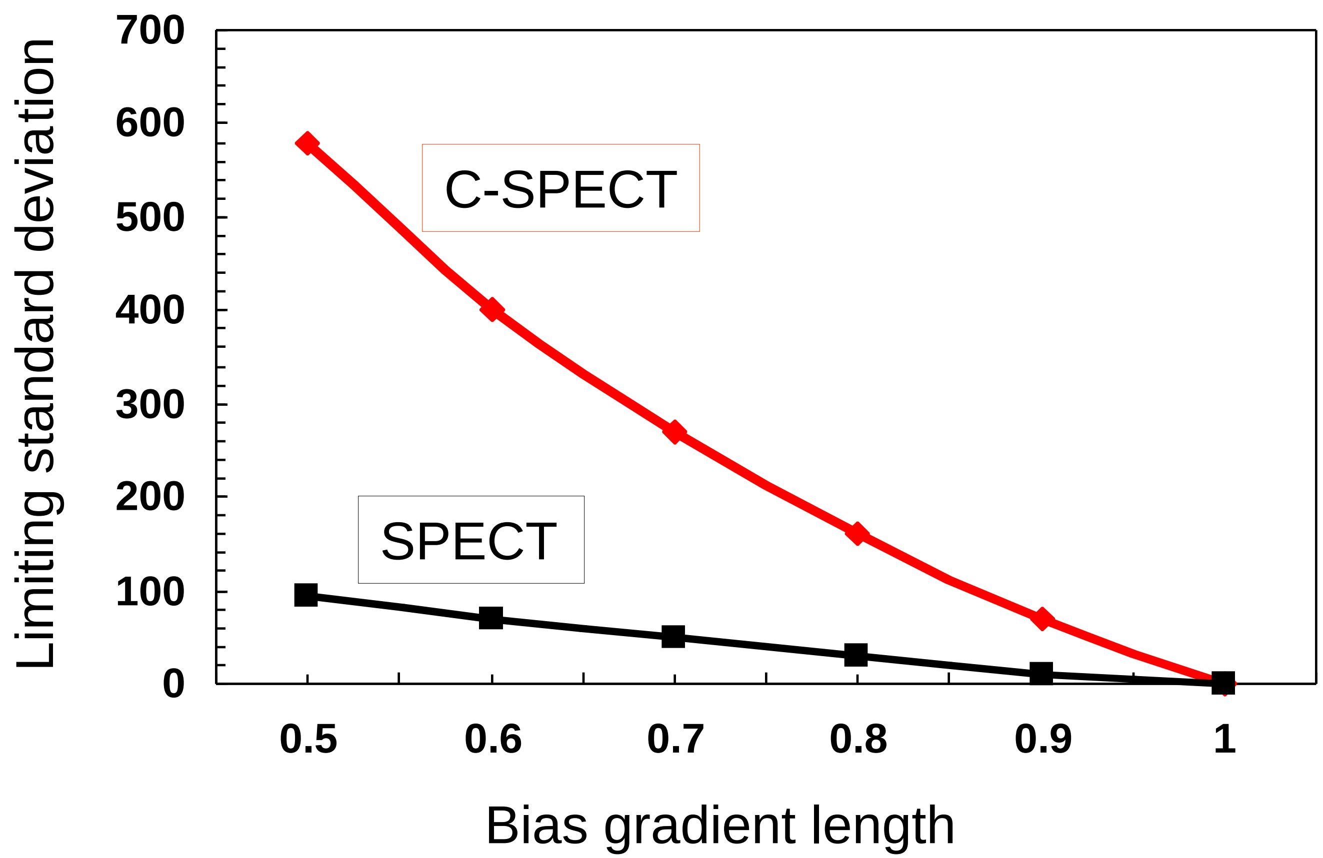

Estimation Performance Comparison with ^{131}I

- Same counts, estimate center pixel of a 7.5cm diameter uniform disk

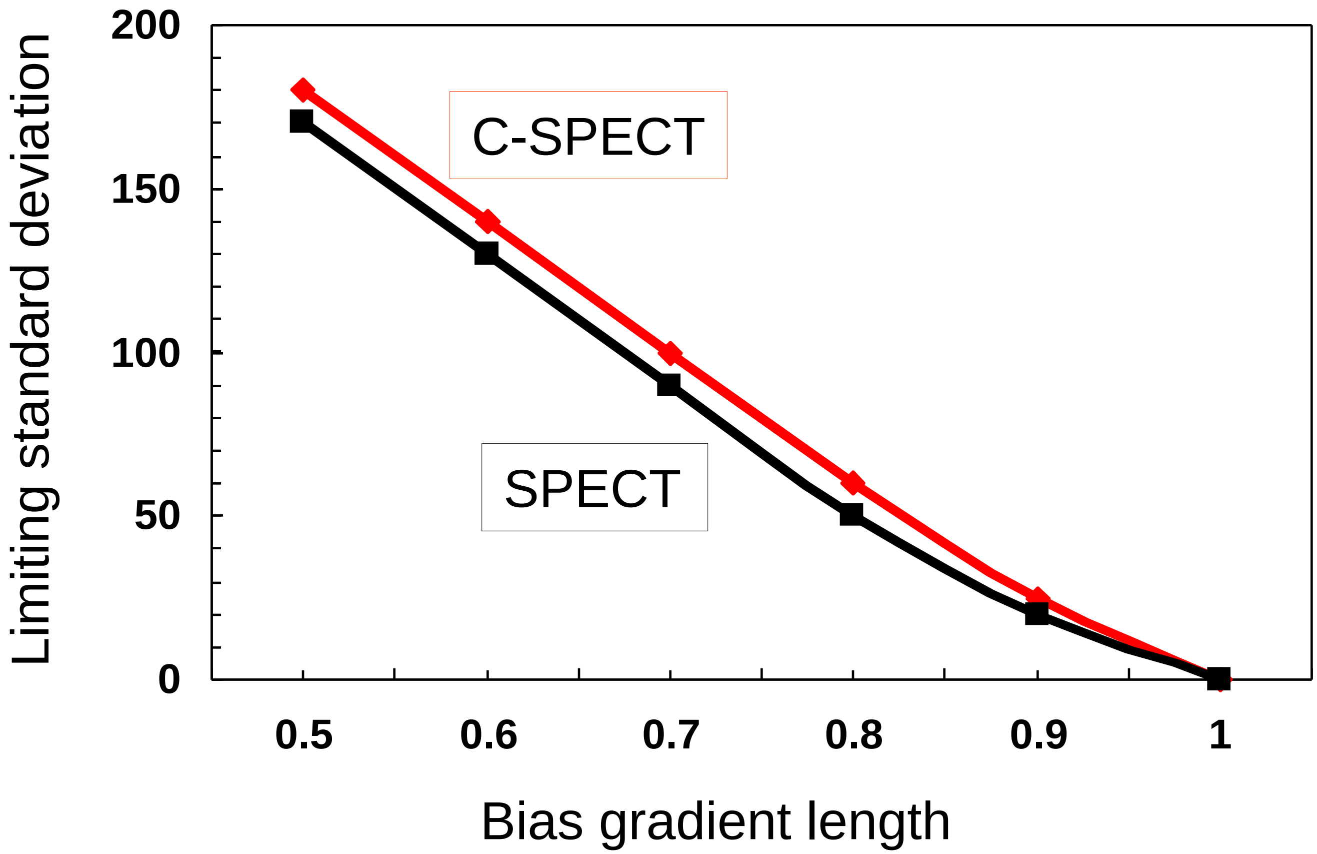

Compton Advantage

- Same imaging time (take efficiency into account)
- Assume a 9x9x0.5 cm^3 silicon 1st-detector (20x efficiency advantage)

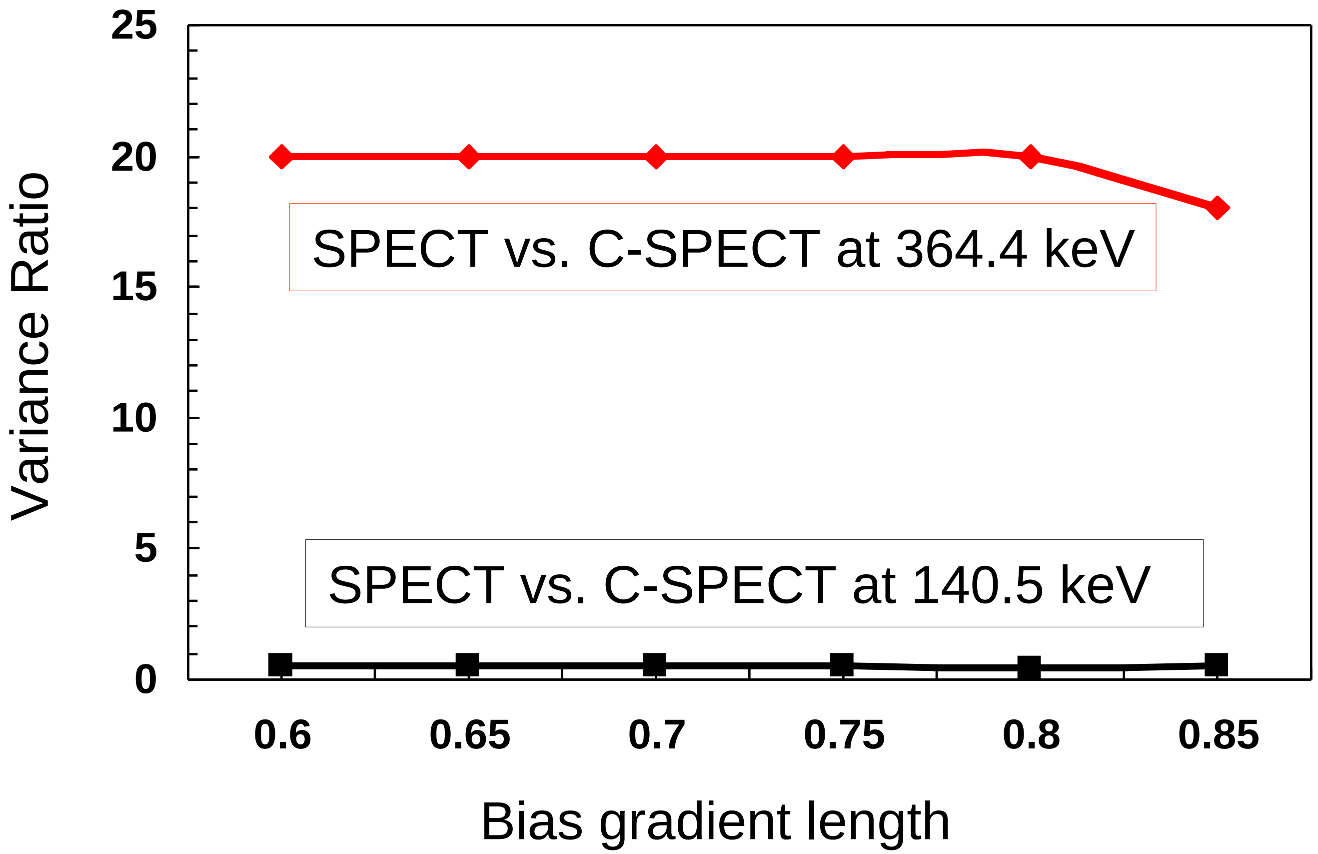

Future Directions

- Fully 3D Tomographic reconstruction
- Binned vs. list-mode acceleration methods
- Experimental verification of bound achievability
- Incorporation of side information